

## Review

## Review of vat photopolymerization 3D printing of photonic devices

Dileep Chekkaramkodi <sup>a,\*</sup>, Liya Jacob <sup>a</sup>, Muhammed Shebeeb C <sup>a</sup>, Rehan Umer <sup>b</sup>, Haider Butt <sup>a,\*</sup><sup>a</sup> Department of Mechanical & Nuclear Engineering, Khalifa University of Science and Technology, P O Box 127788, Abu Dhabi, United Arab Emirates<sup>b</sup> Department of Aerospace Engineering, Khalifa University of Science and Technology, P O Box 127788, Abu Dhabi, United Arab Emirates

## ARTICLE INFO

## Keywords:

Additive manufacturing  
Vat photopolymerization  
3D printing  
Optical devices  
Photonics

## ABSTRACT

Vat photopolymerization (VP) 3D printing, a subset of additive manufacturing, is renowned for its capability to create intricate structures with high precision, particularly useful in optical applications. The process involves using photosensitive resins cured layer by layer through various light-curing technologies like Stereolithography (SLA), Digital Light Processing (DLP), Two-Photon Polymerization (TPP), Continuous Liquid Interface Production (CLIP), and Liquid Crystal Display (LCD). Each technique offers unique advantages in terms of speed, resolution, and material compatibility, with TPP providing the highest resolution. This review explores the diverse applications of VP 3D-printed optical components, including lenses, waveguides, optical gratings, resonators, metamaterials, sensors, and actuators, demonstrating their significant role in advancing optical technology and innovation. Challenges in material selection, post-processing requirements, size limitations, and support structures are discussed, alongside potential future research directions. These include developing advanced photopolymer materials with enhanced optical properties, hardware improvements for higher resolution and multi-material printing, and quality assurance measures for ensuring optical precision. Despite some limitations, VP 3D printing presents a promising avenue for the rapid prototyping and production of complex, multifunctional optical devices, marking a significant stride in optical manufacturing and technological development.

## 1. Introduction

Additive manufacturing (AM) or 3D printing fabricates a complex and monolithic product, layer by layer, which is difficult in conventional manufacturing techniques. The layers are deposited on top of one another until they form the final structure [1]. This process was invented in the 1980 s and is used extensively to build components for various applications because of its low material and energy consumption [2,3]. Furthermore, producing complex geometries is simple and fast, taking only hours instead of weeks compared to conventional processes [4,5]. However, the increased interfaces between the layers lead to reduced mechanical properties. AM is highly beneficial for customizable products and rapid prototyping [6]. The use of AM in optics is investigated by different researchers [7].

Vat photopolymerization (VP) is one of the first and most extensively used 3D printing processes, and it has a considerable impact on a variety of industries [8]. VP involves selectively solidifying liquid resin [9] layer by layer through controlled exposure to light, enabling the precise fabrication of three-dimensional objects with high resolution and complex geometries [10,11]. It employs numerous light-curing technologies

to cure the resin [12]. Depending on the curing light and the method of curing, VP is classified into Stereolithography (SLA), Digital Light Processing (DLP), Two-Photon Polymerization (TPP), Continuous Liquid Interface Production (CLIP), and Liquid Crystal Display (LCD). SLA, DLP, TPP, CLIP, and LCD use laser beams, digital light projectors, concentrated light beams, and continuous liquid interfaces to cure the resin respectively [13]. These 3D printing technologies have distinct advantages in speed, resolution, and material compatibility [11]. Also, functional materials can be integrated within the resin, to create multifunctional products [14,15]. Various materials can be added to VP resin to enhance printability and multifunctionality, including photoinitiators [16] for initiating polymerization upon exposure to light, monomers [17] or oligomers for resin matrix formation [12], ceramics [18,19], solid electroactive particles, soluble components or metal precursors [20] for improved mechanical and electrical properties, and nanoparticles [21–24] for additional functionalities such as conductivity or enhanced material strength.

VP is prominently utilized in industries where precision and intricate detailing are paramount. Commonly employed in manufacturing and prototyping, this 3D printing technology facilitates the rapid creation of

\* Corresponding authors.

E-mail addresses: [100062607@ku.ac.ae](mailto:100062607@ku.ac.ae) (D. Chekkaramkodi), [haider.but@ku.ac.ae](mailto:haider.but@ku.ac.ae) (H. Butt).

prototypes, aiding product development cycles. The dental industry benefits from VP for crafting highly accurate dental models and prosthetics [25]. In jewelry manufacturing, the technology shines by enabling the production of intricate designs with fine details [26]. Aerospace and automotive sectors leverage VP for prototyping complex components [27,28], while the medical field applies it for creating patient-specific models [29], drug delivery, tissue engineering [30], and surgical guides [31]. From consumer goods to footwear, this versatile technology finds applications across various industries, offering a valuable tool for designers, engineers, and manufacturers seeking precision and efficiency in the production of detailed and customized products [10,21,32].

Photonic devices are specialized components used for the manipulation, generation, or detection of light [33]. A few examples of photonic devices include LEDs, Solar and Photovoltaics, displays and optical amplifiers, lenses, and diffraction grating. However, within the scope of VP, polymer-based structures are utilized for the creation of structures and geometries that are capable of manipulation and detection of light [34]. This includes lenses, diffraction grating, optical waveguides, filters, holographic elements, optical fiber-based, and other types of sensors [35–37]. VP 3D printing has been highly beneficial in producing high-quality optical devices because of its high resolution and capability of generating intricate features at the micrometer scale or lower [38]. VP techniques provide better resolution, especially for TPP [39], where the resolution is in the order of nm, which is higher than other types of 3D printing [40]. Aside from its transparency, the versatility of VP is advantageous, allowing for unique design and rapid manufacturing of optical components, making it useful for enormous applications [41]. Grayscale masking, improves its precision, allowing the manufacturing of optical elements with changing refractive indices and complex shapes. VP is critical in efficiently producing optical waveguides, which are essential in data transmission and fiber optics [42,43]. It also provides valuable capabilities for prototyping,

low-volume production, and creating complex, multifunctional optical devices by integrating materials with different optical properties in advancing optical technology and innovation [44].

There had been numerous reviews on the materials and applications of VP [10,12,17–19,21,22,25,28,30,31,45–50]. They deal with different areas of VP, including sensors and actuators using VP, tissue engineering, ceramic VP, challenges with high-speed VP, photoinitiators, and photosensitive inks used in VP. There are some papers previously published in 3D printed photonics. However, as far as our knowledge, there have been no reviews on the optical applications of VP. In this paper, we specifically focus on the current trends of VP 3D printing of optical devices. The first part deals with different types of VP, the second part focuses on the materials used in optical VP, and the third part focuses on different arenas where the optical component of VP is used. The present circumstances of 3D printed photonics are reviewed, and future perspectives and obstacles are also discussed at the end.

## 2. Types of Vat Photopolymerization

### 2.1. Stereolithography

This type of 3D printing was invented by Chuck Hull in 1984 and patented in 1986, as shown in Fig. 1.A [51]. Initially, it is mainly used for rapid prototyping, and a coherent UV laser is used for curing the resin. To get high print speed, galvanometric mirrors are employed to deflect the laser's focus. After completing a layer, the build plate is lowered according to the layer thickness, and then the next layer is printed on the surface of the first one; the process continues until the final shape is achieved [52]. Typically, the 3D printed shape is designed in a CAD file, sliced as needed, and fed into the printer. The spatial resolution of the SLA printer ranges from 25 to 50  $\mu\text{m}$  in the XY plane and 50–100  $\mu\text{m}$  in the Z direction. The XY resolution is limited by the optical diffraction of the printer, and the absorbance of the thickness and

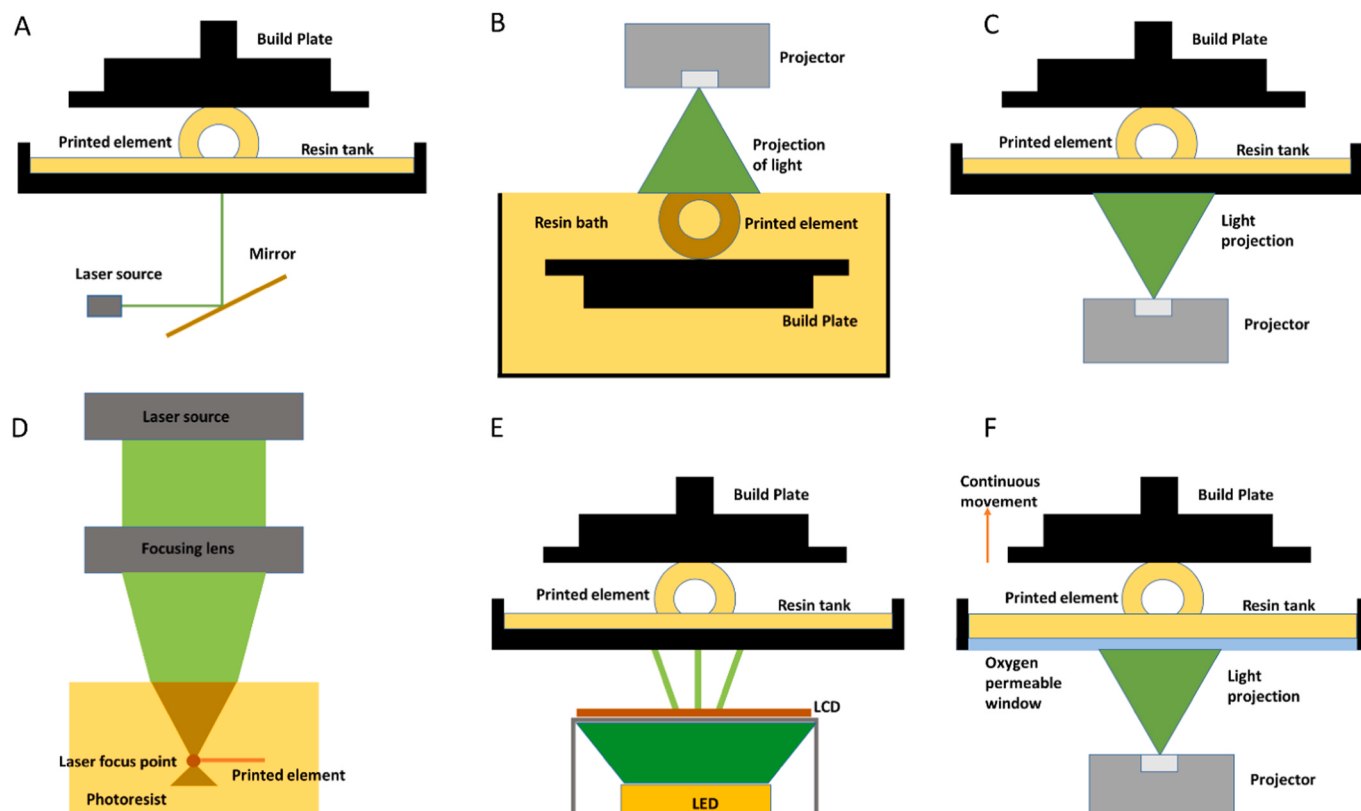


Fig. 1. Different VP printing techniques, A) SLA, B) Top-down DLP, C) Bottom-up DLP, D) TPP, E) LCD, and F) CLIP.

formulation of the print layer limits the Z resolution [53]. Micro stereolithography ( $\mu$ SLA) is a version of SLA that achieves a resolution of 5  $\mu$ m in XY and 10  $\mu$ m in Z by avoiding Gaussian surface imperfections [54]. SLA is used to manufacture a myriad of optical devices, and typically employs a laser to selectively cure liquid resin, producing relatively high irradiance levels centered on specific locations or lines within the resin vat. Since the step effect and edge effect are very common in the final products prepared through stereolithography, post-printing surface treatments are often necessary to obtain smooth surfaces that could be used for photonic applications [55–57].

## 2.2. Digital light processing

A digital micro mirror device (DMD) is utilized in DLP to project the 2D image of the corresponding slice file on the build plate and cure the resin simultaneously, resulting in a higher printing speed than SLA [58]. DLP printers use a digital light projector to expose many layers of resin at once, resulting in homogeneous irradiance across the whole build area. Following the curing of one layer, the build plate rises slightly upwards to pull the model away from the transparent contacting window [59]. The build plate is then moved to the appropriate position, and fresh resin fills the spaces by capillary action. This process will be repeated until the final 3D structure is obtained. DLP printing is classified into two approaches based on the movement of the build plate: top-down and bottom-up [60]. The build plate in the former is entirely immersed in the resin bath, and light is incident on the resin surface, as shown in Fig. 1.B. This approach provides higher spatial resolution, but it consumes a lot of materials [61]. The resin bath's height also limits the print part's height, and controlling the vibration of the resin-air interface is complex. The bottom-up method is suited for mass production, although the resolution is lower than in the other approach shown in Fig. 1.C. It is widely utilized due to its low resin consumption and high leveling rate [62]. The surface difficulties caused by air bubbles created on the surface are the main drawback of this configuration. The XY resolution of the DLP printer is around 10–50  $\mu$ m and is affected by the pixel of the projected light. The vertical resolution is achieved up to 1  $\mu$ m and is affected by the light's penetration into the photocurable resins and curing process. There are several studies reported regarding DLP 3D printing of photonic components [63,64]. Like SLA, step effect and edge effect can arise when printing curved surfaces. Also, since the resin properties could be changed upon the addition of various additives, it is necessary to have optimization in every combination of resin and additives to obtain the best results.

## 2.3. Two-photon polymerization

Two-Photon polymerization, or Direct Laser Writing (DLW), or Two-Photon Absorption (TPA) employs a focused laser beam to cure the photo-resin at the nanoscale [65]. This method has been used to cure photopolymers since the 1960 s and is illustrated in Fig. 1.D. TPP became more popular after introducing susceptible photocurable resins and powerful lasers in the 1990 s [66]. The laser used in TPP has a longer wavelength (often near-infrared) and is unique because it allows for a phenomenon known as "two-photon absorption." Two low-energy photons combine in a compact volume to produce the energy required to commence polymerization [67]. This level of precision enables the fabricating delicate and detailed structures, making TPP excellent for micro-optics and sensing applications [68]. The resolution of this 3D printing technique is about 150 nm, and a high resolution of up to 10 nm is obtained if we use the stimulated emission depletion method in threshold conditions [69–71]. Since the resolution is higher than the wavelength associated with working with visible light, further surface treatment other than washing is often not needed.

## 2.4. Liquid crystal display

LCD is another type of VP process invented by Bertsch et al., in which a dynamic mask generator makes micro parts with complex geometries, as depicted in Fig. 1.E [72]. In other words, the location of the resin solidifies is controlled by the LCD screen, which selectively blocks or enables light to pass through and is shown in Fig. 1. LCD printers, like DLP printers, expose whole layers at once by placing an array of UV lamps or UV LEDs behind an LCD screen, resulting in reasonably consistent irradiance over the build platform. LCD 3D printing is the most commercialized process, and the resolution is about 47  $\mu$ m in horizontal and vertical directions [73–75]. However, further progress is limited due to flaws such as low UV transmission, poor contrast, and high pixel size. A great deal of research is being done to create sophisticated LCD printers. Also, as the DLP and LCD processes are nearly identical, photocurable resins used in DLP are compactable with LCD [76].

## 2.5. Continuous liquid interface production (CLIP)

The continuous liquid interface production utilizes a photosensitive resin which is selectively cured in specific areas while the build plate is moved continuously rather than in steps as in SLA and DLP [77]. The presence of an oxygen-permeable window in CLIP allows oxygen to pass through and control the solidification of resin to achieve the desired result, as shown in Fig. 1.F. By utilizing the continuous printing approach, a superior surface finish and higher production speed is achieved. It shows significant capabilities in producing complex components much more easily, but, the complexity of CLIP restricts its application and requires expertise to perform the task. Shao et al. [78] used CLIP to be able to improve the production speed of optical components compared to their previous microstereolithographic technique. Also, the type of oxygen-permeable window showed significant changes in the surface quality [79]. When the oxygen-permeable window was changed from Teflon to polydimethylsiloxane, due to the changed porosity of permeable membrane, the surface quality was significantly improved. A comparison between different VP techniques are shown in Table 1. a

## 3. Materials used for VP of photonic devices

VP 3D printing operates with photocurable resins; some functional materials are sometimes added to the polymer resin for appropriate properties. This section mainly focuses on different photocurable resins, additives, and binder materials used for printing optical devices for various applications.

### 3.1. Polymers

The transparent polymer resin is the best material for fabricating optical components due to its lightweight, guiding properties, tunable refractive index, and mechanical properties [80]. VP uses photocurable polymer resin to print 3D structures. When these polymers are subjected to specific light wavelengths, usually ultraviolet (UV) or visible light, they are intended to change from liquid or semi-liquid to solid states quickly [81]. To modify the properties of this photocurable resin to suit the requirements, additional monomers or oligomers, functional components, and photoinitiators can be added [82]. The flow properties of the resin depend upon the viscosity. Printing with minute details requires lower viscosity resins, whereas high viscosity resin is used to print large structures without fine details [44,83,84]. The curing characteristics of the polymer also affect the printing speed and precision of the 3D-printed parts; faster curing is required for rapid prototyping applications. In addition, modifying material properties at the molecular level enables the customization of shape, size, and rheological properties to meet the requirements of 3D printing techniques. During the printing

**Table 1**

Comparison between different VP techniques.

Method	Resolution	Surface finish	Volume of printed object	Material	Advantages	Disadvantages	Applications
SLA	25–50 μm	>7 nm	10 <sup>3</sup> –10 <sup>6</sup> cm <sup>3</sup>	Photocurable resin	Print complicated shapes or parts with accuracy	High cost Limited printing area Resin absorb moisture Difficult for multi-material	Lens, Contact lens, Optical fiber, Waveguide
DLP	10–50 μm	>7 nm	10 <sup>3</sup> –10 <sup>6</sup> cm <sup>3</sup>	Photocurable resin	Print complicated shapes or parts with accuracy, Faster for printing large shapes	Limited printing area Resin absorb moisture Difficult for multi-material	Lens, Waveguide, Optical fiber
TPP	Sub- μm	<6 nm	100 × 100 × 8 mm <sup>3</sup>	Photoresist, Photocurable resin	Able to print structures having nanometer dimension	Very slow printing process	Lenses, Fiber tips, etc. have low dimension
LCD	40–50 μm	>10 nm	10 <sup>3</sup> –10 <sup>6</sup> cm <sup>3</sup>	Photocurable resin	Faster compared to SLA	Low resolution	Lens, Optical fiber, Waveguide
CLIP	30–50 μm	>10 nm	10 <sup>3</sup> –10 <sup>7</sup> cm <sup>3</sup>	Photocurable resin	Able to print larger shapes compared to other types of 3D printing High production speed	Printing is complex and needs expertise to operate	Lens, Optical fiber, Waveguide

process, factors such as temperature and heating/cooling rate can influence the microstructures of the printed parts. This includes the size and level of crystallinity, which in turn determine the mechanical and various other characteristics of the printed articles [85].

The most commonly used photocurable polymer is Acrylate-based resin [86]. They are rapid-curing resin, making them suitable for fast prototyping. Their versatility allows them to print both rigid and flexible parts. Polyhydroxymethyl methacrylate (pHEMA), polyethylene glycol diacrylate (PEGDA), and polymethyl methacrylate (PMMA) are some Acrylate based polymers that are widely used for VP 3D printing [87]. SLA and DLP also use epoxy-based polymer resin. Their superior mechanical qualities and resilience to high temperatures make them unique [88]. These resins are frequently used for printing parts for high-temperature applications. Polyurethane-based resins are used for applications requiring high flexibility and elasticity. So, they are primarily used in footwear industries, where flexibility is crucial.

### 3.2. Functional additives

Additives are added to the polymer resin to improve specific properties such as strength, and refractive index, or it is used as a sensing element according to the requirement. Based on the product, these functional materials would be carbon, metal nanoparticles, or ceramics. The introduction of dyes/additives into polymer materials provides substantial advantages by enhancing their capabilities. Even a small amount of dye can greatly modify the material's properties without compromising its mechanical features [89]. Hisham et al. [14] added Atto-dyes into the acrylate polymer resin to filter specific wavelengths for making contact lenses for color blindness correction. These dyes are perfectly dispersed into the polymer resin using a magnetic stirrer and used for printing parts. The final structure has the properties of the polymer and added dyes. The printed parts without dyes transmit all the wavelengths in the visible spectrum, whereas the printed parts with dyes filter specific wavelengths. A DLP 3D printer having a wavelength of 405 nm is used for printing these contact lenses. Alam et al. [87] incorporated thermochromic powders into the photocurable resin and used them for temperature-sensing applications. He added different temperature-sensing powders, which change color according to the temperature, into the photocurable resin and observed that the printed shapes also change color and transmission spectra according to the variation in temperature.

### 3.3. Photoinitiators and coupling agents

Photoinitiators are used to initiate curing reactions in the VP 3D printing process [16]. It is uniformly dispersed into the polymer resin, and once it is exposed to light, it will start cross-linking the polymer chains, resulting in solidification, or curing. Acylphosphine Oxides are

commonly used photoinitiators, which cure quickly and are used to print high-resolution components [90]. Because of their biocompatibility, Iodonium and Sulfonium Salts are also used as photoinitiators for biomedical applications [16]. Camphorquinone is another photoinitiator that initiates a curing reaction at the visible light's lower wavelength [91,92]. Benzoin Ethers initiators provide a slow cure rate; hence, they fabricate components that need precise alignment [93]. Sometimes, a mixture of these photoinitiators is also used for VP printing.

The utilization of white or green-to-NIR light photoinitiating systems for rapid and high-resolution 3D printing remains uncommon compared to prevalent blue/UV light systems [94]. An intriguing avenue for advancement involves a systematic exploration of various organic photoredox dyes, encompassing both commercial and novel synthetically developed dyes not previously employed in 3D printing [95]. The integration of machine learning proves to be invaluable for predicting performance based on reported data, streamlining the selection of photoinitiators within tricomponent systems with minimal experimental efforts [96].

Despite the advantages of reversible addition-fragmentation chain transfer (RAFT)-mediated 3D printing, its print speed and resolution encounter limitations without the incorporation of commercial photoinitiators like diphenyl(2,4,6-trimethylbenzoyl)phosphine oxide (TPO) [97]. The development of more efficient RAFT systems, resistant to oxygen and water interference, is imperative, especially for visible light 3D printing applications such as green light. Preliminary results have been observed, prompting a detailed comparison between RAFT and conventional 3D printing in terms of mechanical properties and cross-linking networks to deepen our understanding of structure–property relationships [98]. Exploring alternative photo-controlled polymerization techniques, such as atom transfer radical polymerization (ATRP), from a distinct chemical perspective could also yield valuable insights.

Coupling agents ensure the uniform dispersion of the functional additives in the polymer resin [99,100]. It also prevents agglomeration of the filler particles in the resin. Silane coupling agents, such as organofunctional silanes, are commonly employed in VP formulations for photonic applications [101]. They can enhance the adhesion and compatibility between different components within the resin. The specific type of silane coupling agent chosen may depend on the nature of the materials in the formulation and the desired properties for photonic applications, such as optical clarity, refractive index control, or other optical functionalities [102].

## 4. Types of VP photonic devices

The VP 3D printed optical device are used for a myriad of applications such as lenses, gratings, waveguides, resonators, metamaterials, sensors, etc. Some post-processing techniques are often used to improve

the properties of 3D-printed objects, especially lenses. Post 3D printing curing or thermal treatment is often done to improve the mechanical properties and polishing the surface is often done to improve the surface quality for better optical devices [103]. There have been a few works where the surface roughness was reduced by a new covering layer of resin material getting cured over the rough surface [104]. Also, Chen et al. [105] and Yuan et al. [106] investigated how grayscale UV exposure could improve surface quality. However, since the presence of additives could vary the properties of the photopolymer resin, deeper knowledge of the 3D printing technique is necessary to obtain the best results.

#### 4.1. Lenses

Optical lenses are clear, curved materials, such as glass, intended to focus and bend light. Lenses are fundamental to many optical instruments, such as telescopes, cameras, microscopes, and eyeglasses. They amplify or improve the clarity of images by bending or refractively entering light until it reaches a point of convergence. Different lenses are used to correct eyesight, capture images, or permit precise observations in sectors like science and astronomy. The unique curvature and shape of a lens determine its optical qualities [107].

Ristok et al. [108] fabricated spherical and non-spherical microlenses by TPP that are comparable with conventional lenses. Fig. 2.A shows the 3D-printed non-spherical and spherical half-ball lenses, and Fig. 2.B depicts the comparison of the printed ball lens with a glass lens.

The lenses exhibit optical design defects caused by photoresist shrinkage, making the larger lens more noticeable. Li et al. [109] manufactured micro objective lenses for ultrathin fiber endoscopes by femtosecond laser-induced TPP method and the SEM images of micro-objective lens are shown in Fig. 2.C. This nanoscale printing process is ideal for realizing complicated micro-optical systems, including aspheric structures. The lenses displayed acceptable imaging performance and offered a novel way to fabricate ultrathin fiber endoscopes. Kiekens et al. [110] utilized a TPP-based 3D printer for preparing a lens of 0.5 mm outer diameter, for use in endoscopes for *in vivo* imaging. Li et al. [111] demonstrated a lens in lens design to achieve high-quality multiple modalities simultaneously. Using TPP, they obtained a miniaturized lens optimized for conflicting modalities such as a high numerical aperture for high-sensitivity fluorescence measurements and a low numerical aperture for achieving depth of field.

Ali et al. [112] investigated the production of holographic Fresnel lenses using a template to create the holographic micrograting on the flat side of a 3D-printed Fresnel lens. They also fabricated high-quality Fresnel lenses with thermochromic dyes using the masked SLA 3D printing method as shown in Fig. 2.D [112]. They added thermochromic materials in the photocurable pHEMA/PEGDA resin, responding to the temperature range of 25–36 °C. Diffraction patterns were imprinted to get holographic diffraction effects at visible to near-infrared wavelengths. They also investigated the effect of wavelength-selective tinted materials in the Fresnel lenses produced by the DLP method [15]. A photosensitive transparent Dentaclear resin was used for this study, and

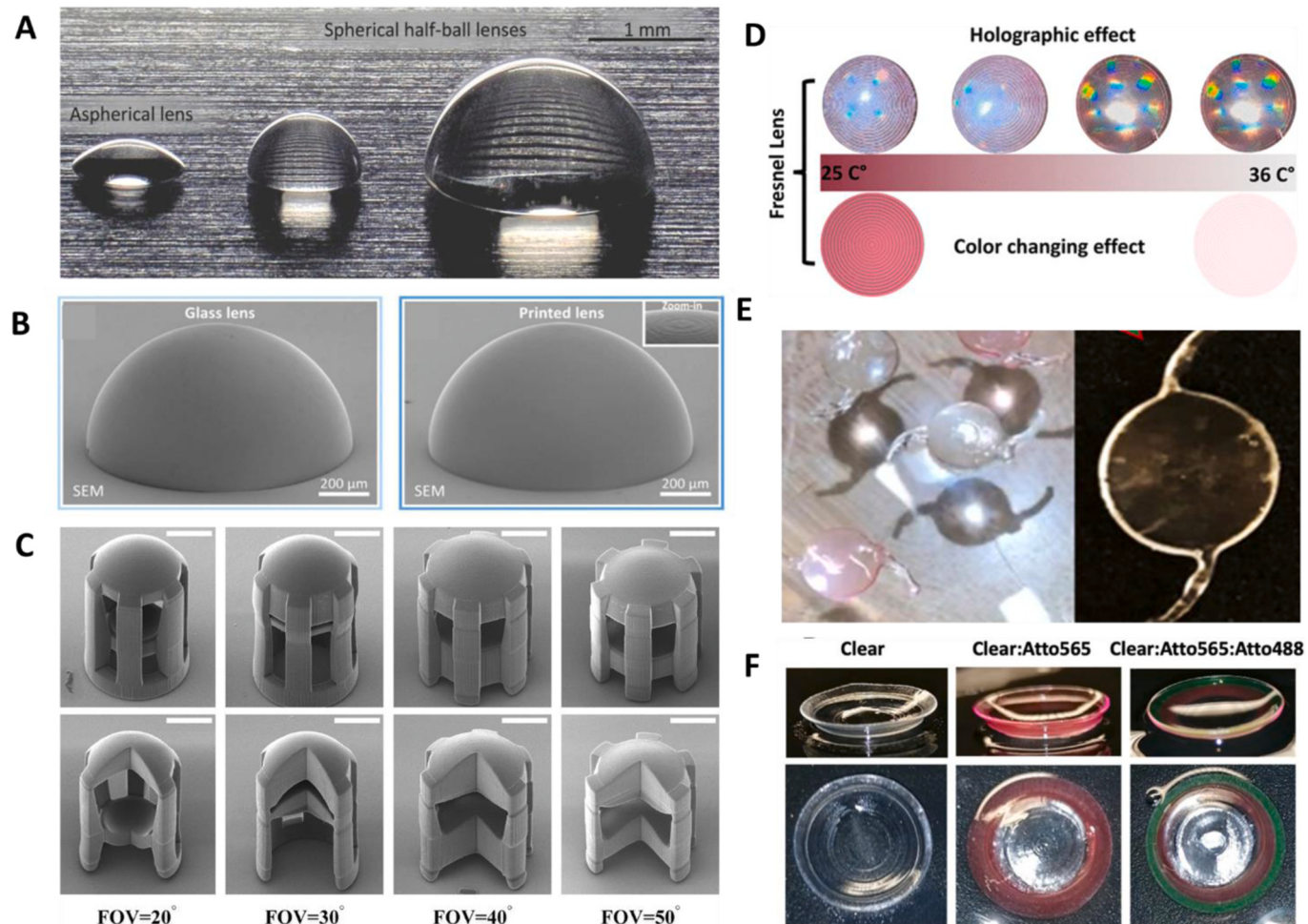


**Fig. 2.** A) TPP 3D printed aspherical lens and half-ball lenses [108], B) SEM images of glass lens and half-ball lens respectively [108], C) SEM images of micro objectives lens at different FOVs and cross-sectional images of micro objective lens at different FOVs [109], D) Color changing Fresnel lens printed by SLA method [112], E) Intraocular lens printed using DLP method [107], and F) multi-material contact lenses printed by DLP method [14].

over 90% transmission was obtained. Also, tinted lenses have a high potential for selective color detection and can be used with wearable devices.

Alam et al. [107] manufactured a 3D-printed intraocular lens for colorblindness correction via DLP, is shown in Fig. 2.E. He used the photosensitive polymer blend of pHEMA and PEGDA for fabricating the intraocular lenses, and Atto-565 dyes were mixed with polymer resin, which filters 50% of the unwanted wavelength of 565 nm, responsible for red-green colorblindness. They also prepared 3D-printed color blindness correction contact lenses using the same combination of materials [113]. The Ishihara test showed enhancement in color perception. Hisham et al. [14] printed multi-material contact lenses with pHEMA/PEGDA resin with Atto-565 dye and pHEMA/PEGDA resin with Atto-488 dye using DLP. Because of the combination of the dyes, the printed multi-material contact lenses provided combined multi-band color blindness correction. The photographs of multi-material contact lenses are shown in Fig. 2.F. The generated optical spectrum was a near match to color blindness corrective glasses that are commercially available.

Other than using a 3D printer to print complete lenses, Salih et al. [114] investigated the capability of using a 3D printer to produce masks that could be used on commercial contact lenses. The masks were utilized to selectively stain part of commercial contact lenses for color blindness correction, such that the tinted area is a small necessary portion and avoid needless attention towards color blindness patients from others.

#### 4.2. Optical gratings

Optical gratings are specialized optical components with grooves or lines spread uniformly across their surface in a periodic pattern [115]. These patterns can diffract light, dividing it into several beams or spreading it into its component colors. Optical gratings play a vital role in many applications, including spectroscopy, in which light is dispersed and analyzed to reveal the properties and composition of substances [116]. They are also employed in optical communication systems to direct and separate light wavelengths. Only a few studies have reported on VP 3D printing of gratings, and the development is in the early stages.

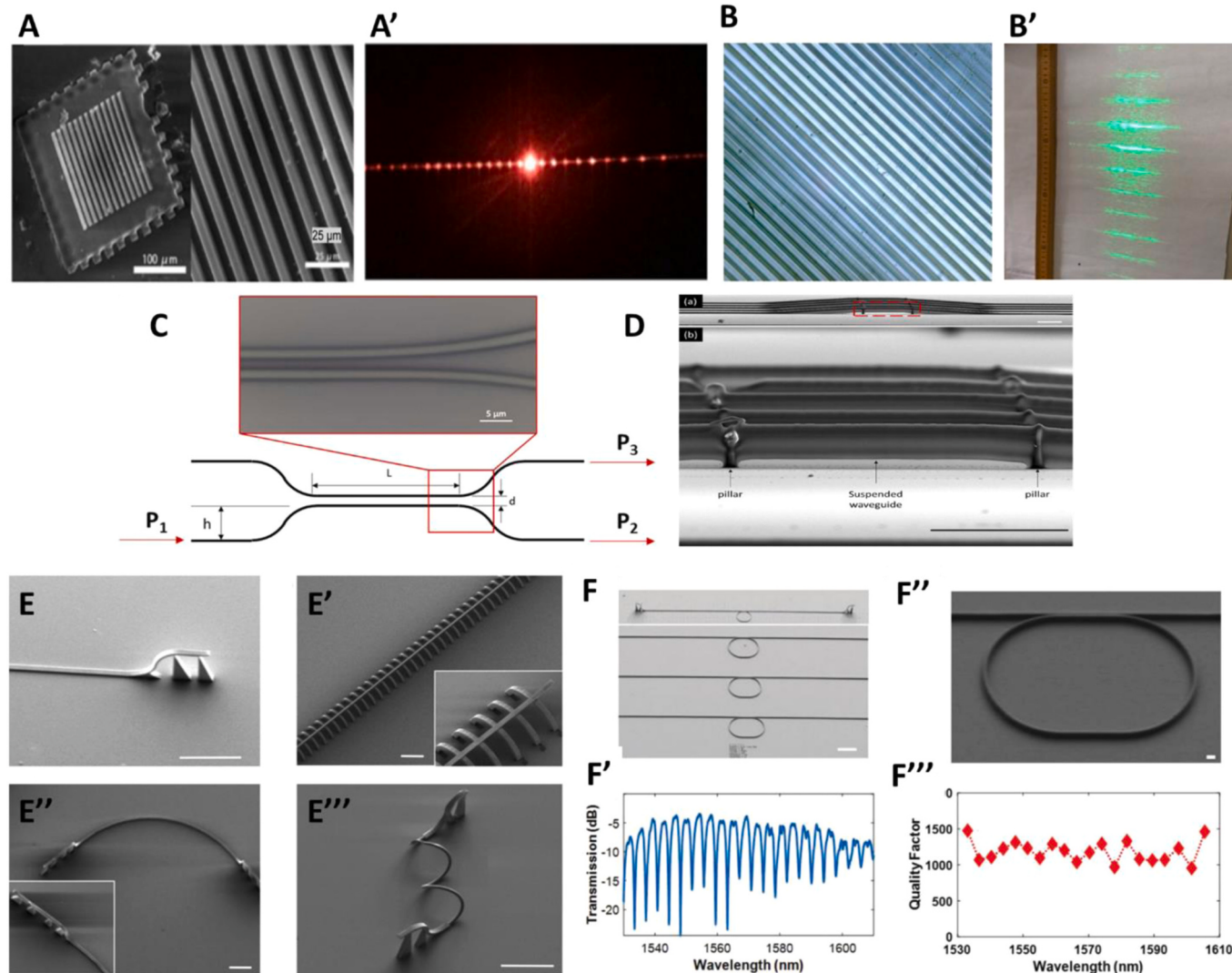


**Fig. 3.** A) SEM images of TPP printed gratings, and A') diffraction pattern of the gratings from a 632.8 nm laser [118], B) optical microscopic image of DLP printed 25  $\mu\text{m}$  grating having magnification 200x, and B') diffraction pattern of the grating [120], C) Schematic diagram of the design and the microscopic image of the directional coupler [124], and D) SEM images of the waveguide produced by TPP method [124], E) SEM images of waveguide-fiber coupling fabricated by TPP, E') waveguide suspended in an arc support, E'') Waveguide printed on the surface of the substrate, and E''') printed 3D spiral waveguide [38], F) and F') are SEM images of ring resonators by TPP printing, F') transmission spectra at different wavelength of the ring resonator and F''') quality factor of the resonators in terms of wavelength [38].

TPP is the most suitable and used method to print optical gratings out of these VP printing methods because of its high resolution [117].

Hong et al. [118] fabricated optical gratings by TPP printer as shown in Fig. 3.A. He used photocurable liquid silica resin with a small fraction of methacryloxy methyltrimethoxysilane as a filler to effectively print the gratings. With a shrinkage rate of 17%, the printed optical elements can be transformed into transparent inorganic glass at temperatures as low as 600 °C. Purtov et al. [119] achieved defect-free pillar arrays with diameters as small as 184 nm using various laser powers near the polymerization threshold of the photoresist. The structures' sizes were compared to theoretical expectations based on Monte Carlo simulations. Optical microscopy was used to examine the optical reflectance of the nanopillar gratings, which was then validated using rigorous coupled-wave simulations. Melgarejo et al. [120] investigated the gratings printed by the DLP method, depicted in Fig. 3.B. They fabricated transmissive gratings with slit separations of 10, 25, and 50 μm. Theoretical irradiance patterns were compared to experimental 3D printed gratings, showing close resemblance in amplitude and peak distances.

#### 4.3. Waveguides

Optical waveguides control and constrain light flow through transparent materials like glass [121]. These waveguides ensure that light stays trapped inside them and travels along a predefined path using the total internal reflection (TIR) concept [122]. The fundamental components of optical communication systems, such as fiber-optic networks, are optical waveguides, which use light pulses to carry data across great distances with lower signal loss. They also play a vital role in several other applications, including laser technology, integrated photonics, and sensing, which allow for the exact manipulation and control of optical signals for various uses [123].

Ng et al. [124] developed a single-mode optical waveguide in SU-8 photoresist using TPP, as shown in Fig. 3.C and D. The waveguide width is increased to reduce coupling loss by scanning the femtosecond laser twice at 0.5 μm intervals. The enhanced waveguide has an 11-decibel insertion loss and a propagation loss of around 1.27 decibels per centimeter. A directional coupler is also built, with 47% and 53% coupling ratios at each port, demonstrating the technique's ability to produce complex waveguide structures such as a vertically hanging waveguide. Gao et al. fabricated a high-resolution optical waveguide using TPP, illustrated in Fig. 3.E [38]. They offer sub-micrometer features and unique coupling interfaces with low coupling losses. Experiment results demonstrate outstanding transmission performance and the capacity to support high-speed data of 30 Gb s<sup>-1</sup> NRZ (non-return to zero) and 56 Gb s<sup>-1</sup>, PAM4 (pulse-amplitude modulation 4) with power penalties of only 0.7 dB for NRZ and 1.5 dB PAM4.

Bertонcini et al. [34] created complicated waveguides from the IP-Dip photoresist using a two-photon lithography procedure and the commercially available Nanoscribe equipment. Using this technology, they constructed a variety of microstructured optical fibers, primarily for an optical mode wavelength of 1060 nm. Examples of these fibers include those with helically twisted hole arrangements, photonic bandgap hollow cores, anti-resonant hollow cores, etc. Frascella et al. [125] utilized a DLP-based 3D printer along with a photoluminescent dye to develop waveguides and splitters to guide the luminescence. The dye's solvatochromic characteristics toward various solvents in the printed structures were preserved by copolymerizing the dye with the polymeric network during the printing process, which permitted the fabrication of solvent polarity sensors.

Schumann et al. [126] demonstrated the usefulness of DLW in integrated optics with instances of its application. They combine the ability to generate a diverse range of 3D polymer structures with well-established production and testing techniques for quasiplanar silicon nitride devices. This technology enables the creation of photonic devices that are difficult to fabricate using typical planar lithography techniques. The researchers demonstrated effective light transmission

from flat rib waveguides to a three-dimensional bridge waveguide, with an insertion loss of less than 2 dB per edge at a wavelength of 1550 nm.

#### 4.4. Resonators

Optical resonators, or optical cavities, are critical components in laser systems and other optical devices [127]. These resonators capture and circulate light within a small space, usually between two highly reflective mirrors or surfaces. The trapped light is reflected several times, creating standing waves and amplifying specific optical frequencies. This resonance effect is critical in laser technology because it creates coherent and bright light.

Gao et al. [38] fabricated a high-resolution ring resonator by using TPP printing, which is shown in Fig. 3.F. Li et al. [128] printed a highly integrative optofluidic refractometer based on tubular optical microcavities coupled with waveguides by TPP. Through fiber taper coupling, such tubular devices can support high-quality factor (Q-factor) up to 3600. A 390 nm/refractive index unit (RIU) sensitivity is observed under a liquid-in-tube sensing configuration with a subwavelength wall thickness of 0.5 μm, providing a detection limit of around 10<sup>-5</sup> RIU. Liu et al. [129] investigated the viability of utilizing TPP to directly write zirconium/silicon hybrid sol-gel to produce high-quality factor ( $1.48 \times 10^5$ ) polymer whispering gallery microcavities. He achieved a surface roughness below 12 nm, enabling the pathway to 3D print intricate microcavities for making optical resonators. Li et al. [130] 3D printed whispering gallery mode (WGM) resonators on a microfiber by femtosecond laser TPP method. The typical resonance was detected by connecting the microresonator to a tapered fiber where they were physically apart. This photosensitive resin-based resonator was placed on a microfiber, which increased structural integration in contrast to typical WGM devices. This device is handy for measuring temperature, with a maximum sensitivity of 1.68 nm/°C and a Q-factor of  $1.9 \times 10^3$ . Zhang et al. fabricated high-quality factor WGMs with various materials, which show excellent sensitivity to biocomponents, gases, and nanoparticles [131]. The smooth surface finish of the fabricated structure is responsible for the high Q-factor.

The major challenge in using VP for printing resonators is achieving the necessary precision for intricate resonator structures, as the layer-by-layer approach may compromise the fabrication of complex optical components [132]. Ensuring manufacturing efficiency and structural integrity remains a concern, as layer-wise construction may result in slower build speeds and potential performance limitations. Additionally, optimizing the process for fabricating multicomponent optical resonators demands overcoming challenges associated with equipment complexity and high costs, hindering widespread adoption for advanced optical applications [133].

#### 4.5. Metamaterials

Optical metamaterials are artificial materials with unique and exotic properties. They are designed at the nanoscale and feature complicated structures that manipulate light in unconventional ways, such as bending it in peculiar directions or exhibiting negative refractive indices. Optical metamaterials are promising for many applications, including optical cloaking, super-resolution imaging, and developing high-performance lenses and antennas. VP printing of metamaterials is a little tricky, and TPP is the best method to print these structures due to its high resolution. Thus far, it has yet to be possible to fabricate superior metallic 3D structures with TPP. The most feasible method to fabricate metamaterials entails precisely creating dielectric structures and metalizing them after fabrication [134]. The complex process of achieving the requisite metamaterial properties at optical frequencies necessitates resolution, appropriate metallization, and careful material selection.

Xu et al. [135] developed a VP 3D printing for printing diverse micro-architectures containing numerous internally suspended features,

extensive overhangs, and struts with high aspect ratios. This innovative method eliminates the necessity for manually removing internal supports, opening the door to a range of multi-functional metamaterials with various designed properties. These properties include wide bandgaps for elastic waves at low frequencies, switchable wave transmissions, and the creation of products that require no post-support removal. The synthesis and rapid printing of a variety of metamaterials with a broad array of suspended features are detailed, showcasing their metamaterial behaviors. This approach removes limitations related to scale and unit cells, enabling the incorporation of embedded features across multiple materials. Fig. 4 shows the printed parts and their optical band gap performance. Kim et al. [136] developed functionally graded materials (FGMs) using a cost-effective single-vat DLP method. Two innovative approaches were employed: graded AM, manipulating polymerization through varying brightness, and selective post-curing based on functional requirements. The combination of these

methods allows for the development of FGMs with contradictory properties—high surface hardness and flexural flexibility. These hard yet flexible metamaterials can be used in novel functional structures, eliminating the need for additional coatings or assembly processes. Lu et al. [137] formed ultraviolet (UV)-curable polysiloxane (PSO) resin slurry using VP based on computer simulation technology (CST), a gyroid structure (GS) with excellent formability and high ceramic yield. Upon pyrolysis at temperatures between 1100–1300 °C, the resulting GS SiOC metamaterials exhibited a density range of  $1.430 \sim 1.612 \text{ g}\cdot\text{cm}^{-3}$ , showcasing a minimum reflection loss ( $\text{RL}_{\min}$ ) of  $-59.96 \text{ dB}$  at 2.90 mm and an effective absorption bandwidth (EAB) spanning 4.20 GHz (8.2–12.4 GHz) at thicknesses ranging from 2.69–3.15 mm, covering the entire X-band electromagnetic wave spectrum. The simulated reflection loss (RL) results for the GS metamaterials align with experimental values at various thicknesses.

VP poses several challenges in the precise printing of optical

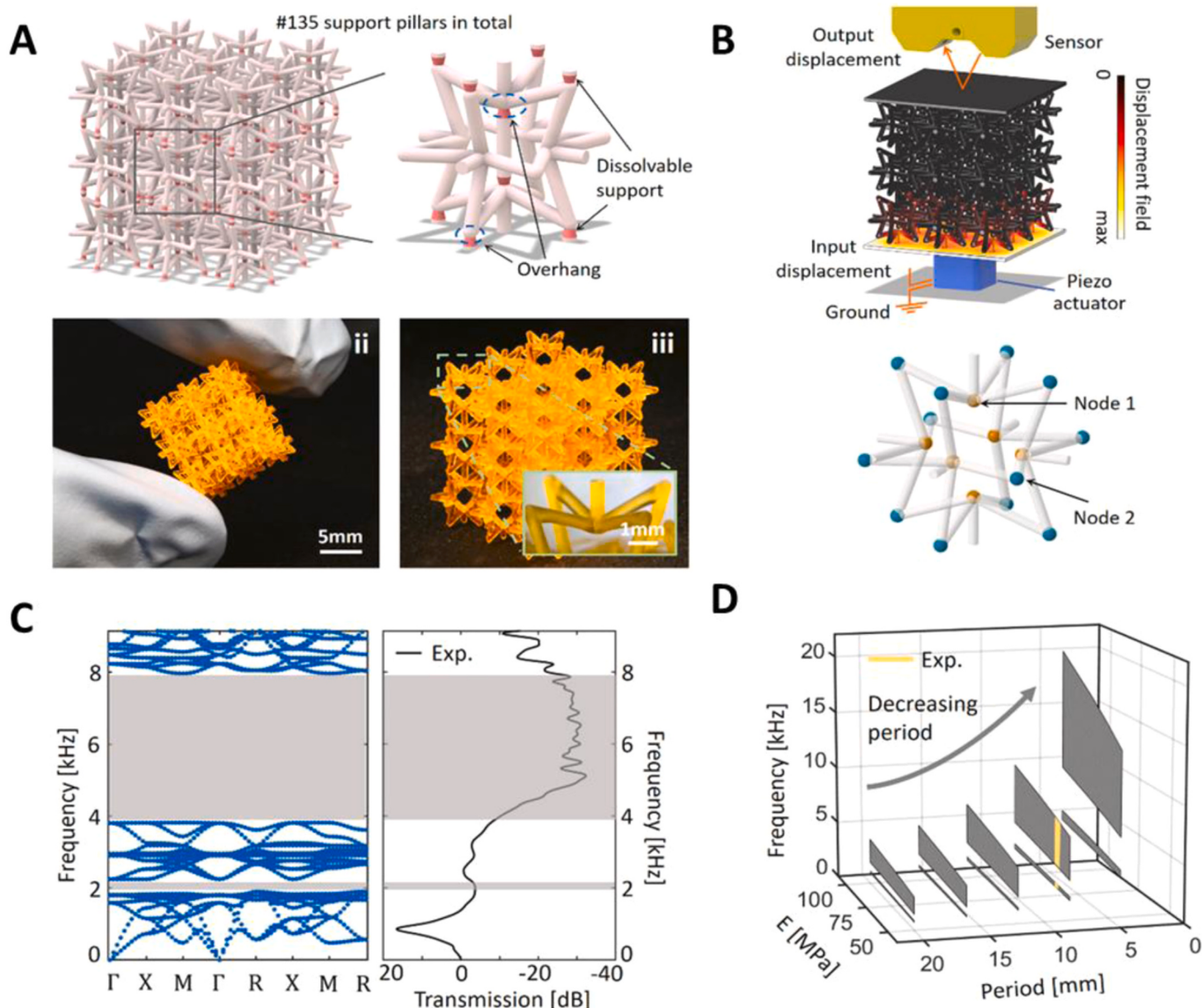


**Fig. 4.** A) star-shaped re-entrant lattice, comprising a designed lattice with 135 internal support pillars. The circled area indicates the overhanging section requiring support, and the pink sections represent the dissolvable material. B) The 3D-printed lattice made of Bisphenol A ethoxylate dimethacrylate (BPAEDA) and trimethylpropane triacrylate (TMPTA) is depicted after the removal of supports. The schematic of the measurement platform includes two different nodes of the star-shaped unit cell, with side plates from the same material for testing convenience. C) The lattice's numerical results for the normalized displacement field at 6 kHz frequency are presented. D) The band structure and measured elastic wave transmission via the lattice are showcased, with shaded grey regions indicating band gaps. Accessing larger frequency range bandgaps is demonstrated by decreasing the structure's period and adjusting the stiffness of the base materials, with a period of 8 mm and elastic modulus of 62.3 MPa for the sample [135].

metamaterials, especially for advanced applications. Achieving manufacturing efficiency and structural integrity remains a primary concern, as the layer-by-layer approach often results in slower build speeds and inferior performance compared to traditional formative processes like injection molding. The limited availability of functional materials suitable for VP 3D printing hinders the fabrication of optical metamaterials, particularly those with intricate optical properties. The insufficiency of high-conductive polymer materials for electrodes, in

comparison to conventional metal materials, presents a critical obstacle in realizing the desired optical functionalities [138]. Developing multicomponent optical devices using VP 3D printing requires overcoming challenges related to bulky equipment, complex operating systems, and high costs, which may impede widespread adoption in academic settings. Also, the application of VP 3D printing to produce optical metamaterials for biological electronics introduces challenges in optimizing materials for biocompatibility while maintaining the desired

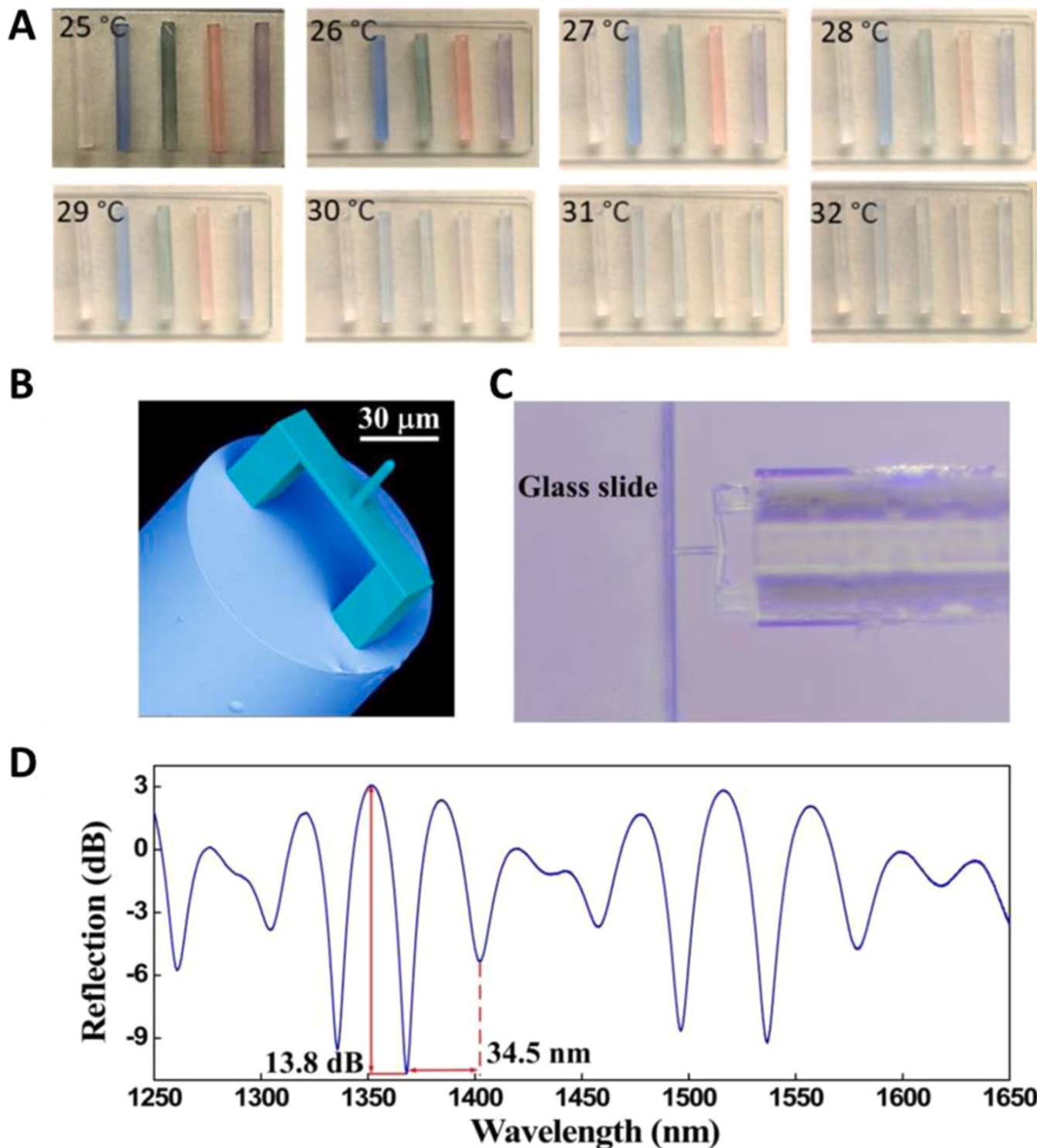


**Fig. 5.** A) The color changes of DLP printed thermochromic optical fiber probes at various temperature [87], B) SEM image of fabricated FTMS, C) Photograph of FTMS pressed on the edge of glass slide, D) FTMS reflection spectrum [145].

optical properties, necessitating a careful balance between functionality and biological responsiveness [139]. Addressing these challenges is crucial for advancing the capabilities of VP in printing optical metamaterials for cutting-edge research.

#### 4.6. Sensors and actuators

One of the most significant requirements in engineering is the measurement of various parameters such as force, strain, temperature, pressure, displacement, etc., and various sensors are fabricated and tested for this purpose [1]. A variety of mechanical and electrical sensors are employed for measuring these parameters. However, they exhibit limitations under certain environmental conditions, such as susceptibility to electromagnetic interference and a tendency to malfunction under extreme load conditions [140]. One of the main alternatives to these traditional sensors are photonic sensors, which exhibit excellent electromagnetic interference resistance, corrosion resistance, high signal-to-noise ratio, long life (>20 years), and lightweight [141] [142]. As a result, optical sensors are appealing to the industry. These optical sensors' sensing capacity or sensitivity is heavily influenced by the material properties, manufacturing resolution, homogeneity, and interfacial uniformity. As a result, 3D printing is the best choice since it provides excellent resolution, layer-by-layer material monitoring, and greater interfacial homogeneity [60].

Shen et al. [143] fabricated a fiber-optic Fabry-Perot interferometer (FPI) based fiber optic sensor using the DLP method for water pressure sensing. The interference contrast is increased by an eight-degree angle on the optical fiber end face and obtains a sensitivity of 536.9 nm/MPa. Alam et al. [87] printed a nanocomposite optical fiber in different orientations by DLP for temperature sensing, is shown in Fig. 5.A. They used thermochromic powders as the sensing element, which changes color based on temperature variations. To investigate the thermal response of the components, reflection spectra are recorded in the visible wavelength range, and some variations in the spectra at different temperatures. They also investigated the strain-sensing capacity of the device by bending the fabricated fiber at 45° and 90° angles.

Poduval et al. [144] manufactured a sensing service for intravascular pressure sensing, and it is incorporated in the face of single-mode optical fiber. The active components of the sensor featured a pressure-sensitive diaphragm and an intermediate temperature-sensitive spacer that was unaffected by variations in external pressure. The deflection of the diaphragm and the thermal expansion of the spacer in proportion to the fiber end-face were measured using phase-resolved low-coherence interferometry. This fiber optic sensor could detect pressure fluctuations as little as 0.38 mmHg in the 760–1060 mmHg (absolute pressure) range and temperature variations as small as 0.023 °C in the 25–47 °C range. This technology can potentially speed up the creation of a wide range of fiber-optic sensors with pressure and temperature sensitivity, which might be used to guide less invasive surgical procedures. Zou et al. [145] 3D printed a fiber tip micro-force (FTMS) sensor using the TPP method for measuring interfacial adhesion force, is depicted in Fig. 5.B, C and D. A clamped-beam probe was built on the tip of a single-mode fiber to create this gadget and a sensitivity of 1.05 nm/N and resolve forces as low as 19 nN was achieved. The sensor was used as part of a regular validation approach to measuring both contact and noncontact adhesion forces at the micronewton level, particularly on the surfaces of hydrogels.

The synergy of fabrication systems in VP and polymer materials, possessing stretchability, biocompatibility, and self-healing abilities, aligns with the development trends in soft sensor and actuator devices. The potential for a fully developed wearable soft electronic system is envisioned to enable health monitoring, diagnostics, and continuous treatment. Challenges include improving manufacturing efficiency, expanding the range of accessible functional materials, simplifying the development of multicomponent devices, and addressing concerns related to biological electronics [27]. Additional considerations involve

enhancing the composite performance, robustness, and aesthetics of soft robotics applications, as well as ensuring user customization for wearable and implantable devices. Despite challenges, VP 3D printing is anticipated to be a disruptive innovation revolutionizing the fabrication and integration of soft electronic devices.

### 5. Effect of optical properties of the materials on print quality

#### 5.1. Refractive index

In VP, the refractive index of the material affects printing quality. It is mainly because of its effect on optical clarity, indicating the degree of transparency and light scattering within the resin during the printing process [146]. Alignment between the refractive indices of the resin, build platform, and light source becomes important for achieving uniform curing depths, thereby ensuring consistency in part strength and dimensions. Moreover, this also enhances printing resolution and detail by enabling precise focusing of light within the resin, resulting in sharper features and smoother surfaces.

Liang et al. [146] demonstrated the importance of refractive index on the print quality of a material. When using opaque instead of translucent filler material, the curing characteristics also depend on light absorption, i.e., the filler scatters and absorbs light but does not transmit it through the filler. Hence, an opaque filler blocks light to the photopolymer behind it, whereas a translucent filler allows light to pass through and cure the photopolymer, which explains the different results. The opacity of the filler and its refractive index determine the fraction of incident light that passes through the material, which directly influences the resulting object. These results are in agreement with Martin et al. [147] and Choong et al. [148]. However, they contrast the results presented by, e.g., Xu et al., [149] who used opaque instead of translucent filler material, and documented that the curing depth decreases with increasing filler fraction.

Zhang et al. [150] found that there is a linear relationship between the refractive index of a material and the degree of curing when used in VP. Although a basic linear model demonstrates reasonable effectiveness within a defined range of depth of cure (DoC), its utility is circumscribed by delineated boundaries shaped by the intricate interplay with the material's density, refractive index, and additional properties such as molecular-level structures. A correlation model between refractive index and depth of cure (DoC) is devised through curve fitting using the DoC and refractive index values from the initial two replications in each sample set, as illustrated in Fig. 6. The resultant fitted correlation model is expressed as  $\text{DoC} = 16.934 - 24.963$ , with a coefficient of determination ( $R^2$ ) of 0.8523. Subsequently, the efficacy of this estimated correlation model is evaluated on previously unseen data, specifically the third replication within each sample set. The average error across all five samples is found to be 16.2%. This study adopts a linear model for correlation establishment, akin to Howard et al. [151]. Notably, Fig. 6 reveals that beyond a DoC of 50%, the change in refractive index with increasing DoC becomes relatively insignificant. It's important to acknowledge that the limited sample size may have a notable impact on model development and accuracy. Nevertheless, the observation in Fig. 6 aligns with findings from Aloui's investigation on the refractive index evolution in a series of commercial acrylic resins during photopolymerization [152].

#### 5.2. Absorptivity

In VP, print quality is influenced by various factors, including the absorptivity of the photopolymer resin. Absorptivity refers to the material's ability to absorb light, which plays a significant role in the curing process during printing. A resin's absorptivity affects the curing depth, resolution, and surface finish of the printed object, ultimately impacting the overall quality of the print. Balancing the light source intensity with the resin's absorptivity is crucial for achieving precise and consistent

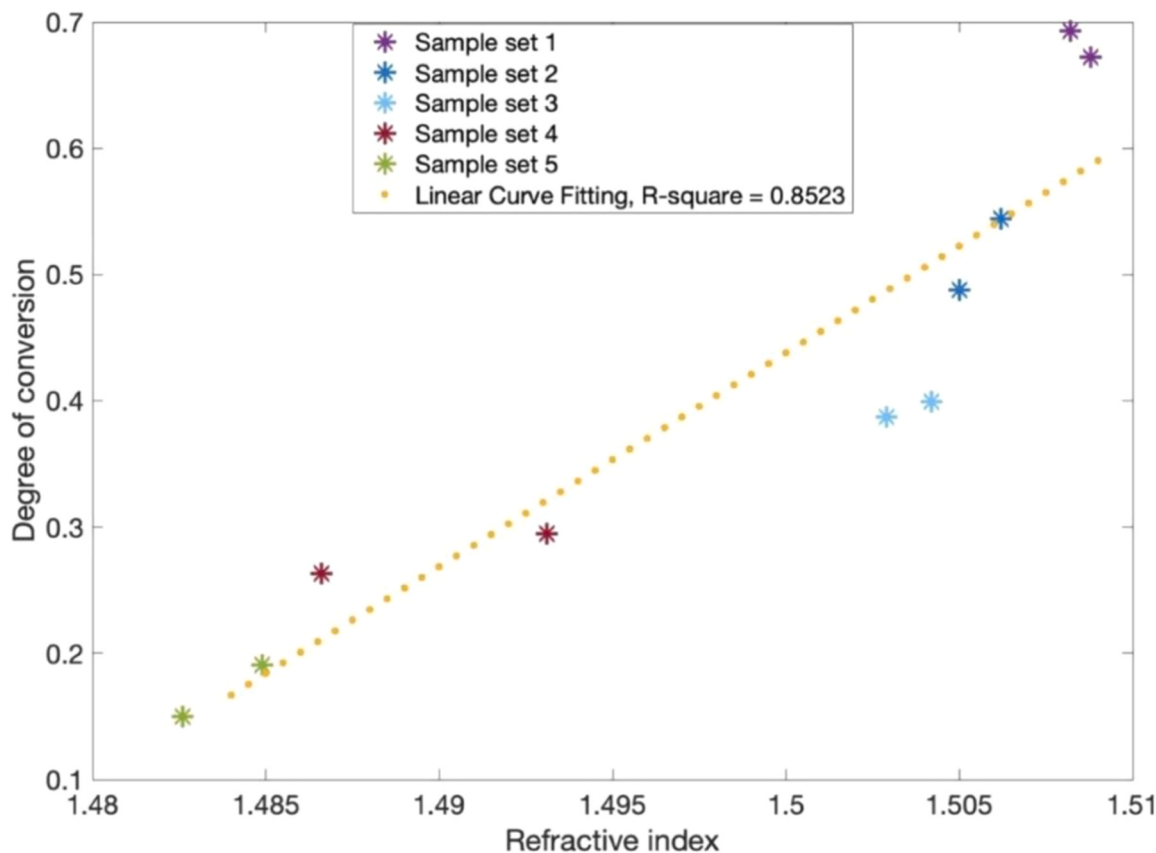


**Fig. 6.** Correlation model of refractive index and DoC[150].

results.

Wang et al. [153] introduced a mathematical model based on the Beer-Lambert Law (BLL) to analyze how the depth of light penetration in a resin affects molar absorptivity in relation to light dose. The model considers concentrations of substances such as monomers, free radicals, photoinitiators, and light absorbers, which are key components in the reaction process[154]. Research by Gong et al. [155] [155] demonstrated how adjusting molar absorptivity and the concentration of various monomers can optimize microfluidic features, while Li et al. [156] showed how varying concentrations of light absorbers influence the photopolymerization process. As the concentration of light absorbers increases, curing threshold and efficiency decrease. By applying a tunable threshold during the pre-curing stage, high-fidelity and high-efficiency continuous printing can be achieved. The Beer-Lambert Law, a fundamental principle in photochemistry and spectroscopy, describes how the absorption of monochromatic light decreases exponentially as it passes through a light-absorbing material[157]. This law states that the absorbance of light is directly proportional to the concentration of the absorbing species and the path length that the light travels through the material. In the context of vat photopolymerization, the law helps in understanding how light penetration depth in a resin affects the curing process. As light travels through the resin, it is absorbed by photoinitiators and other substances, leading to a decrease in light intensity with increasing thickness of the resin. This relationship is crucial for controlling and optimizing the curing process in 3D printing to achieve precise and consistent prints [153].

## 6. Post-processing of 3D printed optical devices to remove step effect and surface roughness

Post-processing is an important step to reduce the roughness associated with the step effect and pixelation derived from the 3D printer.

Post-surface treatment such as polishing or introducing a smoother layer over the 3D printed surface has been investigated. Xu et al. utilized LCD-based volumetric projection stereolithography to produce miniature lenses with micrometer form error and sub-nanometer roughness [104]. After printing the pixelated structure using the 3D printer, the residual resin film was re-cured to achieve a smoother surface. An iterative learning model was utilized to achieve the desired shape of the final product as the residual resin film control is needed for the best result. This method was utilized to reduce the step effect associated with the layer by deposition. Meniscus recoating was also investigated to achieve a better surface finish for the 3D-printed lenses. However, the improvement was hugely dependent upon the wetting behavior of lenses, and the dimensions of steps/plateau associated with the design and is often highly difficult to control. The schematics of this work are represented in Figures 6.7. Chen et al. utilized grayscale UV exposure to improve the surface quality along with meniscus recoating. A combination of meniscus recoating and grayscale projection 3D printing was able to achieve a better surface finish of 7 nm surface roughness. Fig. 7.C represents the manufactured lens and its use for high-resolution imaging [105]. Yuan et al. utilized an oscillation-assisted DLP printer to eliminate jagged surfaces formed by discrete pixels and a 1–3 seconds single grayscale exposure to remove the staircase effect [106]. Fig. 7.A represent the changes in surface roughness using SEM, AFM, and optical images. Alam et al. reduced the step effect in a 3D printed contact lens by dip-coating a layer of resin over the surface.

Sun et al. [61] investigated the possibility of utilizing stereolithography to make packaging for phosphor-coated WLEDs. They employed post-processing polishing to reduce the surface roughness. Similarly, Aguirre et al. [62] utilized aluminum oxide micro-graded polishing paper to grind the 3d printed spherical and aspherical lenses. Zhang et al. [63] developed a 3D printing method that involves the use of a continuous liquid film to create highly precise 3D structures,

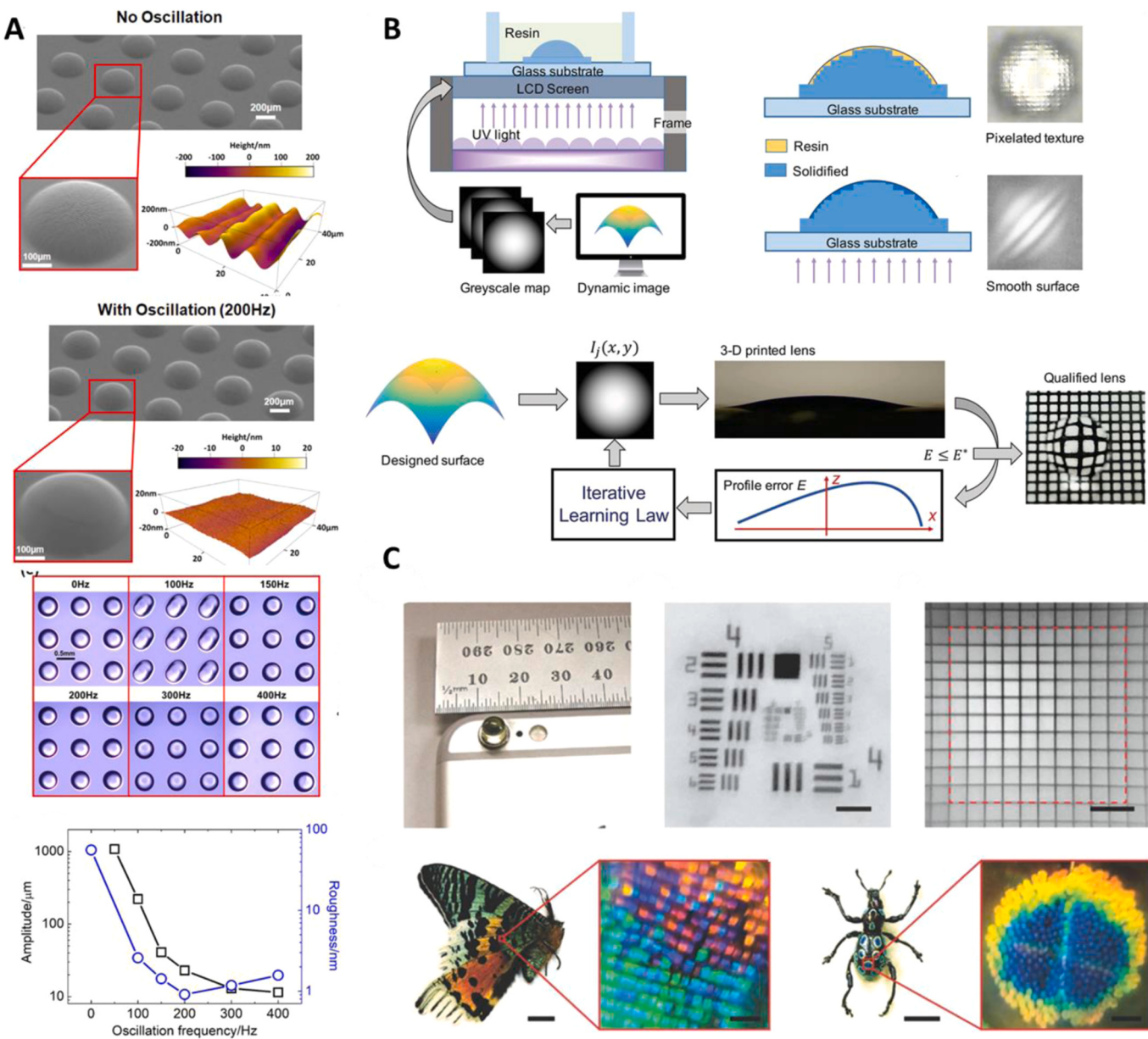


**Fig. 7.** A) SEM and AFM results of the micro-lens produced under nonoscillated and oscillated projection. Top view pictures of micro-lens produced under elevated oscillation frequencies. Relationship between the current setup's oscillation frequency and amplitude and the resulting impact on the manufactured micro-lenses' surface roughness [106]. B) Iterative learning-based volumetric projection stereolithography- The printer arrangement, the printed structure featuring a pixelated texture and resin film that is bonded to the printed surface, and the leftover resin film's re-polymerization to produce an optically smooth surface (the strips represented illumination light pictures), and the lens accuracy improvement iterative learning technique, where  $E$  and  $E^*$  represent the permitted and practical profile errors, respectively [104]. C) Cost effective optical imaging using a printed aspheric lens. Pictures of an aspheric lens connected to a mobile camera. Images taken by the mobile camera through a printed lens, including, Groups 4–7 in a USAF 1951 resolution test chart (200 μm-scale bar), A grid pattern (500 μm-scale bar), pictures of multicolored sample, images of a Madagascan sunset moth (20 mm-scale bar), photographs of the moth's wing captured by the camera with a printed aspheric lens (500 μm-scale bar), images of a weevil *Pachyrhynchus congestus* (5 mm-scale bar), images of a single spot on the weevil's elytra by mobile camera with a printed aspheric lens (500 μm-scale bar) [105].

utilizing DLP technology. Through the management of the interface between the liquid and solid materials and the adoption of a continuous printing approach, the excess liquid resin that attaches to the cured structure is drawn into the cured layer structures, effectively eliminating any unwanted step artifacts and negating the necessity for post-printing cleaning processes. It is like CLIP however, an oxygen-permeable layer is absent.

Shao et al. [78] utilized a micro continuous liquid interface printing along grayscale photopolymerization and meniscus coating to improve the production time and surface quality of optical components. Also, the

change of oxygen permeable window from Teflon membrane with micrometer size pores to polydimethylsiloxane with nanoscopic pores could improve the surface quality and achieve a roughness of around 13.7 nm. The final 3D printed 3 mm aspherical lens which was printed in 2 mins, demonstrated imaging resolution of 3.10 μm.

Additional methods for post-treatment include mechanical polishing and the application of enhanced resins. Mechanical polishing typically involves the use of polishing papers by hand or with automated machinery. Heinrich et al. [158] described employing a six-axis robot to maneuver the polishing tool over the optical surface according to a

predetermined path. Kowsari et. al investigated the effects of various types and concentrations of in-house developed (meth)acrylate-based photopolymer components on the quality and resolution of structures fabricated using a bottom-exposure DLP-based 3D printing system. They examined different resin compositions to determine the most efficient ones for attaining the best printing precision and surface smoothness while considering a variety of mechanical characteristics. Their study demonstrated the exact fabrication of sub-pixel conical and aspherical smooth features, with the ability to customize both shape and dimensions through the use of specific resin formulas and process settings [159].

The layer-by-layer manufacturing process employed in VP results in intrinsic anisotropy in the finished products, which is a serious concern. Although anisotropy can affect the mechanical properties of printed parts, its impact on optical properties is far more significant, particularly when designing and manufacturing optical components. Non-uniform optical performance can be caused by changes in refractive index, transparency, and light scattering behavior in different directions inside the printed material. Differences in optical properties can cause distortions, aberrations, and uneven light transmission through the component, significantly reducing its functionality and reliability in optical systems. To overcome this issue, carefully consider the materials used, printing conditions, and post-processing processes. This is required to limit the appearance of anisotropic effects and ensure the consistent and reliable performance of optical components made using VP methods. In addition, Glass optical components are well-known for their remarkable durability and reliability, which make them ideal for a variety of applications. Printed polymers and photo-polymers tend to age over time. Prolonged exposure to external variables including light, heat, and humidity can impair material properties, making it difficult to maintain consistent performance and reliability. As a result, careful thought and mitigation methods are required when using printed polymers and photopolymers in optical systems to assure their long-term functioning and performance.

## 7. Challenges and future aspects

There are many challenges in fabricating optical components by the VP process. The major problems are listed below:

- Materials: Compared to other manufacturing methods, the choice of photopolymer resins available for VP can be limited. It might be challenging to find materials that meet specific optical requirements, such as refractive indices, dispersion properties, or spectrum transmission. Some photopolymer materials may exhibit scattering or birefringence, which may have an impact on the optical performance of the final structure.
- Post-processing: VP provides excellent resolution and surface finish; some optical components may require post-processing procedures like polishing or coating to fulfill the appropriate optical criteria. These extra stages might complicate and lengthen the manufacturing process.
- Size limitations: In VP printing, the physical size of the vat or build volume might limit the size of optical components that can be made.
- Supports: VP is ideal for producing complicated geometries with great precision; highly intricate or overhanging structures sometimes necessitate support structures that must be removed post-printing.

Despite these challenges, several future research areas can be explored in the VP 3D printing process. Which include:

- Development of advanced materials: New photopolymer materials with advanced optical properties, such as high refractive indices, reduced dispersion, and better environmental stability, can be developed through research, which broadens the applications for VP printed optical devices.

- Hardware development: Advances in 3D printing technology, such as resolution improvements and the creation of suitable light sources, will help to ensure the effective production of high-quality optical components. Developing methods for simultaneous printing with different materials, each with unique optical properties can lead to the fabrication of complex optical components with specific features.
- Quality assurance and monitoring: Develop high-precision measurement procedures and quality control systems for VP 3D-printed optical components to ensure they fulfill rigorous optical criteria. In addition, real-time monitoring and feedback systems during the printing process detect and fix problems that may impair optical quality, hence decreasing rework and wastage of materials.
- Dispersion of functional element: The agglomeration and settlement of added functional materials pose some issues. This results in an obstruction to the propagation of light waves.

By addressing these issues, it can fully utilize VP 3D printing to manufacture optical components.

## 8. Conclusions

VP is distinguished by its exceptional high-resolution capabilities, making it well-suited for demanding optical applications requiring intricate structures at micrometer sizes. Out of these VP printing techniques, TPP provides excellent resolution, but it is comparatively expensive. On the other hand, SLA, DLP, and LCD are cost-effective but give low printing resolution. The transparency of photosensitive resin is critical for effective light transmission across a wide range of wavelengths, meeting the needs of photonic devices. Furthermore, the viscosity, curing properties of the resin, and dispersed functional elements influence the behavior of the final photonic devices. Although the review highlights several noteworthy benefits of VP 3D-printed optical components, it also underscores limitations such as lack of advanced materials, inefficient dispersion of functional elements, etc. Overall, the adaptability of VP allows for the personalized design and rapid prototyping of optical components, which is critical in research and development areas.

## CRediT authorship contribution statement

**Dileep Chekkaramkodi:** Writing – original draft, Validation, Software, Methodology, Data curation, Conceptualization. **Liya Jacob:** Writing – original draft, Investigation. **Muhammed Shebeeb C:** Writing – original draft. **Haider Butt:** Writing – review & editing, Supervision, Resources, Project administration. **Rehan Umer:** Writing – review & editing, Supervision.

## Declaration of Competing Interest

The authors declare that they have no known competing financial interests or personal relationships that could have appeared to influence the work reported in this paper

## Data Availability

Data will be made available on request.

## Acknowledgements

The authors acknowledge Sandoog Al Watan LLC for the research funding (SWARD Program—AWARD, Project code: 8434000391-EX2020-044). We also acknowledge Khalifa University of Science and Technology for the research funding (Award No. RCII-2019-003) in support of this research.

## References

- [1] M.R. Khosravani, T. Reinicke, 3D-printed sensors: current progress and future challenges, *Sens. Actuators A: Phys.* 305 (2020) 111916.
- [2] D. Bekas, et al., 3D printing to enable multifunctionality in polymer-based composites: a review, *Compos. Part B: Eng.* 179 (2019) 107540.
- [3] M.R. Khosravani, T. Reinicke, On the environmental impacts of 3D printing technology, *Appl. Mater. Today* 20 (2020) 100689.
- [4] M. Hisham, et al., Additive manufacturing of carbon nanocomposites for structural applications, *J. Mater. Res. Technol.* 28 (2024) 4674–4693.
- [5] J. Jiang, X. Xu, J. Stringer, Optimization of process planning for reducing material waste in extrusion based additive manufacturing, *Robot. Comput.-Integr. Manuf.* 59 (2019) 317–325.
- [6] I. Campbell, D. Bourrell, I. Gibson, Additive manufacturing: rapid prototyping comes of age, *Rapid Prototyp. J.* 18 (4) (2012) 255–258.
- [7] A. Camposeo, et al., Additive manufacturing: applications and directions in photonics and optoelectronics, *Adv. Opt. Mater.* 7 (1) (2019) 1800419.
- [8] K. Rooney, et al., Additive manufacturing in Australian Small to medium enterprises: vat polymerisation techniques, case study and pathways to industry 4.0 competitiveness, *J. Manuf. Mater. Process.* 7 (5) (2023) 168.
- [9] J.F.P. Lovo, et al., Vat photopolymerization additive manufacturing resins: analysis and case study, *Mater. Res.* 23 (2020).
- [10] F. Zhang, et al., The recent development of vat photopolymerization: a review, *Addit. Manuf.* 48 (2021) 102423.
- [11] M. Pagac, et al., A review of vat photopolymerization technology: materials, applications, challenges, and future trends of 3d printing, *Polymers* 13 (4) (2021) 598.
- [12] A. Al Rashid, et al., Vat photopolymerization of polymers and polymer composites: processes and applications, *Addit. Manuf.* 47 (2021) 102279.
- [13] H. Quan, et al., Photo-curing 3D printing technique and its challenges, *Bioact. Mater.* 5 (1) (2020) 110–115.
- [14] M. Hisham, A.E. Salih, H. Butt, 3D printing of multimaterial contact lenses, *ACS Biomater. Sci. Eng.* (2023).
- [15] M. Ali, et al., 3D printing of Fresnel lenses with wavelength selective tinted materials, *Addit. Manuf.* 47 (2021) 102281.
- [16] Y. Bao, Recent trends in advanced photoinitiators for vat photopolymerization 3D printing, *Macromol. rapid Commun.* 43 (14) (2022) 2200202.
- [17] S.K. Paral, et al., A Review of critical issues in high-speed vat photopolymerization, *Polymers* 15 (12) (2023) 2716.
- [18] I.L. de Camargo, et al., A review on the rheological behavior and formulations of ceramic suspensions for vat photopolymerization, *Ceram. Int.* 47 (9) (2021) 11906–11921.
- [19] X. Wu, et al., Research progress of the defects and innovations of ceramic vat photopolymerization, *Addit. Manuf.* (2023) 103441.
- [20] A. Maurel, et al., Toward high resolution 3D Printing of shape-conformable batteries via vat photopolymerization: Review and perspective, *IEEE Access* 9 (2021) 140654–140666.
- [21] M. Shah, et al., Vat photopolymerization-based 3D printing of polymer nanocomposites: current trends and applications, *RSC Adv.* 13 (2) (2023) 1456–1496.
- [22] A. Medellin, et al., Vat photopolymerization 3d printing of nanocomposites: a literature review, *J. Micro-Nano-Manuf.* 7 (3) (2019) 031006.
- [23] Y. Li, et al., Vat polymerization-based 3D printing of nanocomposites: A mini review, *Front. Mater.* 9 (2023) 1118943.
- [24] L.D. Gil, et al., Systematic overview of nanocomposites obtained by VAT photopolymerization techniques: A cost and life cycle assessment approach, *Rev. UIS Ing.* 12 (2) (2023).
- [25] L. Andjela, et al., A review on Vat Photopolymerization 3D-printing processes for dental application, *Dent. Mater.* (2022).
- [26] F. Cooper, Do the new, low-cost photopolymer 3D printers now becoming available have a place in the jewelry manufacturing environment, *St. Fe Symp. Jewel. Manuf. Technol.* (2016).
- [27] W. Zhao, et al., Vat photopolymerization 3D printing of advanced soft sensors and actuators: From architecture to function, *Adv. Mater. Technol.* 6 (8) (2021) 2001218.
- [28] R.V. Pazhamannil, P. Govindan, Current state and future scope of additive manufacturing technologies via vat photopolymerization, *Mater. Today.: Proc.* 43 (2021) 130–136.
- [29] D. Bahati, M. Bricha, K. El Mabrouk, Vat photopolymerization additive manufacturing technology for bone tissue engineering applications, *Adv. Eng. Mater.* 25 (1) (2023) 2200859.
- [30] N.A. Chartrain, C.B. Williams, A.R. Whittington, A review on fabricating tissue scaffolds using vat photopolymerization, *Acta Biomater.* 74 (2018) 90–111.
- [31] X. Xu, et al., Vat photopolymerization 3D printing for advanced drug delivery and medical device applications, *J. Control. Release* 329 (2021) 743–757.
- [32] I. Gibson, et al., Vat photopolymerization processes, *Addit. Manuf. Technol.: 3D Print., rapid Prototyp., Direct Digit. Manuf.* (2015) 63–106.
- [33] S.L. Chuang, Physics of photonic devices, John Wiley & Sons, 2012.
- [34] A. Bertoncini, C. Liberale, 3D printed waveguides based on photonic crystal fiber designs for complex fiber-end photonic devices, *Optica* 7 (11) (2020) 1487–1494.
- [35] Y. Jiang, et al., Recent advances in 3D printed sensors: materials, design, and manufacturing, *Adv. Mater. Technol.* 8 (2) (2023) 2200492.
- [36] A. Lambert, S. Valiulis, Q. Cheng, Advances in optical sensing and bioanalysis enabled by 3D printing, *ACS Sens.* 3 (12) (2018) 2475–2491.
- [37] Q. Sun, et al., Stereolithography 3D printing of transparent resin lens for high-power phosphor-coated WLEDs packaging, *J. Manuf. Process.* 85 (2023) 756–763.
- [38] H. Gao, et al., High-resolution 3D printed photonic waveguide devices, *Adv. Opt. Mater.* 8 (18) (2020) 2000613.
- [39] A. Hayat, et al., Applications of two-photon processes in semiconductor photonic devices: invited review, *Semicond. Sci. Technol.* 26 (8) (2011) 083001.
- [40] H.Y. Jeong, et al., 3D and 4D printing for optics and metaphotonics, *Nanophotonics* 9 (5) (2020) 1139–1160.
- [41] A.M. Al-Amri, Recent Progress in Printed Photonic Devices: A Brief Review of Materials, Devices, and Applications, *Polymers* 15 (15) (2023) 3234.
- [42] H. Ramollari, P. Measor, A low-loss 3D printed ridge waveguide via stereolithography, in: *Integrated Optics: Devices, Materials, and Technologies XXVI*, SPIE, 2022.
- [43] Shen, J., et al. *Rapid prototyping of low loss 3D printed waveguides for millimeter-wave applications.* in: *2017 IEEE MTT-S International Microwave Symposium (IMS)*. 2017. IEEE.
- [44] P.F. Jacobs, Rapid prototyping & manufacturing: fundamentals of stereolithography, Society of Manufacturing Engineers, 1992.
- [45] A. Andreu, et al., 4D printing materials for vat photopolymerization, *Addit. Manuf.* 44 (2021) 102024.
- [46] U. Shaukat, E. Rossegger, S. Schlögl, A review of multi-material 3D printing of functional materials via vat photopolymerization, *Polymers* 14 (12) (2022) 2449.
- [47] I. Sachdeva, et al., Computational AI models in VAT photopolymerization: a review, current trends, open issues, and future opportunities, *Neural Comput. Appl.* 34 (20) (2022) 17207–17229.
- [48] S. Nohut, M. Schwentenwein, Vat photopolymerization additive manufacturing of functionally graded materials: a review, *J. Manuf. Mater. Process.* 6 (1) (2022) 17.
- [49] T. Hafkamp, et al., A feasibility study on process monitoring and control in vat photopolymerization of ceramics, *Mechatronics* 56 (2018) 220–241.
- [50] C.M. Sheebib, et al., Vat photopolymerisation 3D printing of graphene-based materials, *Virtual Phys. Prototyp.* 18 (1) (2023) e2276250.
- [51] C.A.G. Lengua, History of rapid prototyping, *Rapid Prototyp. Card. Dis.: 3D Print. Heart* (2017) 3–7.
- [52] E.M. Maines, et al., Sustainable advances in SLA/DLP 3D printing materials and processes, *Green. Chem.* 23 (18) (2021) 6863–6897.
- [53] U. Kalsoom, P.N. Nesterenko, B. Paull, Current and future impact of 3D printing on the separation sciences, *TrAC Trends Anal. Chem.* 105 (2018) 492–502.
- [54] J. Stampfl, et al., Photopolymers with tunable mechanical properties processed by laser-based high-resolution stereolithography, *J. Micromech. Microeng.* 18 (12) (2008) 125014.
- [55] J.R.C. Dizon, et al., Post-processing of 3D-printed polymers, *Technologies* 9 (3) (2021) 61.
- [56] I. Karakurt, L. Lin, 3D printing technologies: techniques, materials, and post-processing, *Curr. Opin. Chem. Eng.* 28 (2020) 134–143.
- [57] W. Piedra-Cascón, et al., 3D printing parameters, supporting structures, slicing, and post-processing procedures of vat-polymerization additive manufacturing technologies: A narrative review, *J. Dent.* 109 (2021) 103630.
- [58] J. Zhang, et al., Digital light processing based three-dimensional printing for medical applications, *Int. J. Bioprinting* 6 (1) (2020).
- [59] G. Varghese, et al., Fabrication and characterisation of ceramics via low-cost DLP 3D printing, *Boletín De la Soc. Española De Cerámica Y. Vidr.* 57 (1) (2018) 9–18.
- [60] H. Gao, et al., 3D printed optics and photonics: Processes, materials and applications, *Mater. Today* (2023).
- [61] O. Santoliquito, P. Colombo, A. Ortona, Additive Manufacturing of ceramic components by Digital Light Processing: A comparison between the “bottom-up” and the “top-down” approaches, *J. Eur. Ceram. Soc.* 39 (6) (2019) 2140–2148.
- [62] J.-C. Wang, M. Ruilova, Y.-H. Lin, The development of an active separation method for bottom-up stereolithography system, *2017 IEEE/SICE International Symposium on System Integration (SII)*, IEEE, 2017.
- [63] R. Gvishi, I. Sokolov, 3D sol-gel printing and sol-gel bonding for fabrication of macro-and micro/nano-structured photonic devices, *J. Sol.-Gel Sci. Technol.* 95 (2020) 635–648.
- [64] J. Liao, et al., 3D-printable colloidal photonic crystals, *Mater. Today* 56 (2022) 29–41.
- [65] M. Mao, et al., The emerging frontiers and applications of high-resolution 3D printing, *Micromachines* 8 (4) (2017) 113.
- [66] J.-F. Xing, M.-L. Zheng, X.-M. Duan, Two-photon polymerization microfabrication of hydrogels: an advanced 3D printing technology for tissue engineering and drug delivery, *Chem. Soc. Rev.* 44 (15) (2015) 5031–5039.
- [67] Q. Geng, et al., Ultrafast multi-focus 3-D nano-fabrication based on two-photon polymerization, *Nat. Commun.* 10 (1) (2019) 2179.
- [68] J. Li, et al., Two-photon polymerisation 3D printed freeform micro-optics for optical coherence tomography fibre probes, *Sci. Rep.* 8 (1) (2018) 14789.
- [69] X. He, et al., STED direct laser writing of 45 nm width nanowire, *Micromachines* 10 (11) (2019) 726.
- [70] S. Juodkazis, et al., Two-photon lithography of nanorods in SU-8 photoresist, *Nanotechnology* 16 (6) (2005) 846.
- [71] Z. Gan, et al., Three-dimensional deep sub-diffraction optical beam lithography with 9 nm feature size, *Nat. Commun.* 4 (1) (2013) 2061.
- [72] A. Bertsch, et al., Microstereolithography using a liquid crystal display as dynamic mask-generator, *Microsyst. Technol.* 3 (2) (1997) 42–47.
- [73] W. Shan, et al., 4D printing of shape memory polymer via liquid crystal display (LCD) stereolithographic 3D printing, *Mater. Res. Express* 7 (10) (2020) 105305.

- [74] A. Sotov, et al., LCD-SLA 3D printing of BaTiO<sub>3</sub> piezoelectric ceramics, *Ceram. Int.* 47 (21) (2021) 30358–30366.
- [75] R. Oliveira, R. Nogueira, L. Bilro, 3D printed long period gratings and their applications as high sensitivity shear-strain and torsion sensors, *Opt. Express* 29 (12) (2021) 17795–17814.
- [76] I.A. Tsolakis, et al., Comparison in terms of accuracy between DLP and LCD printing technology for dental model printing, *Dent. J.* 10 (10) (2022) 181.
- [77] D.E. Düzgün, K. Nadolny, Continuous liquid interface production (CLIP) method for rapid prototyping, *J. Mech. Energy Eng.* 2 (1) (2018) 5–12.
- [78] G. Shao, R. Hai, C. Sun, 3D printing customized optical lens in minutes, *Adv. Opt. Mater.* 8 (4) (2020) 1901646.
- [79] K. Taki, A simplified 2D numerical simulation of photopolymerization kinetics and oxygen diffusion–reaction for the continuous liquid interface production (CLIP) system, *Polymers* 12 (4) (2020) 875.
- [80] G. Taormina, et al., 3D printing processes for photocurable polymeric materials: technologies, materials, and future trends, *J. Appl. Biomater. Funct. Mater.* 16 (3) (2018) 151–160.
- [81] E. Geisler, M. Lecompte, O. Soppera, 3D printing of optical materials by processes based on photopolymerization: materials, technologies, and recent advances, *Photonics Res.* 10 (6) (2022) 1344–1360.
- [82] A.J. Ruiz, et al., 3D printing fluorescent material with tunable optical properties, *Sci. Rep.* 11 (1) (2021) 17135.
- [83] R.H. Bean, et al., Rheology guiding the design and printability of aqueous colloidal composites for additive manufacturing, *J. Vinyl Addit. Technol.* 29 (4) (2023) 607–616.
- [84] I. Gibson, et al., Additive manufacturing technologies, Vol. 17, Springer, 2021.
- [85] X. Zhang, et al., Immunomodulatory Microneedle Patch for Periodontal Tissue Regeneration, *Mater* 5 (2) (2022) 666–682.
- [86] A. Navaruckiene, et al., Vanillin acrylate-based resins for optical 3D printing, *Polymers* 12 (2) (2020) 397.
- [87] F. Alam, et al., 3D printed polymer composite optical fiber for sensing applications, *Addit. Manuf.* 58 (2022) 102996.
- [88] L. Pezzana, et al., Hot-lithography 3D printing of biobased epoxy resins, *Polymer* 254 (2022) 125097.
- [89] M. Gastaldi, et al., Functional Dyes in Polymeric 3D Printing: Applications and Perspectives, *ACS Mater. Lett.* 3 (1) (2021) 1–17.
- [90] Y. Wu, et al., New acyl phosphine oxides as high-performance and low migration type I photoinitiators of radical polymerization, *Prog. Org. Coat.* 168 (2022) 106876.
- [91] F. Li, et al., Rapid additive manufacturing of 3D geometric structures via dual-wavelength polymerization, *ACS Macro Lett.* 9 (10) (2020) 1409–1414.
- [92] M. Topa, et al., One-component cationic photoinitiators based on coumarin scaffold iodonium salts as highly sensitive photoacid generators for 3D printing IPN photopolymers under visible LED sources, *Polym. Chem.* 11 (32) (2020) 5261–5278.
- [93] E. Hola, M. Pilch, J. Ortyl, Thioxanthone derivatives as a new class of organic photocatalysts for photopolymerisation processes and the 3D printing of photocurable resins under visible light, *Catalysts* 10 (8) (2020) 903.
- [94] W. Qiu, et al., Polymerizable oxime esters: an efficient photoinitiator with low migration ability for 3D printing to fabricate luminescent devices, *ChemPhotoChem* 4 (11) (2020) 5296–5303.
- [95] M. Elbadawi, et al., Disrupting 3D printing of medicines with machine learning, *Trends Pharmacol. Sci.* 42 (9) (2021) 745–757.
- [96] G.D. Goh, S.L. Sing, W.Y. Yeong, A review on machine learning in 3D printing: applications, potential, and challenges, *Artif. Intell. Rev.* 54 (1) (2021) 63–94.
- [97] S. Ye, et al., Continuous color tuning of single-fluorophore emission via polymerization-mediated through-space charge transfer, *Sci. Adv.* 7 (15) (2021) eabd1794.
- [98] Y. Bao, J. Nicolas, Structure–cytotoxicity relationship of drug-initiated polymer prodrug nanoparticles, *Polym. Chem.* 8 (34) (2017) 5174–5184.
- [99] J.-G. Jang, et al., Evaluation of Physical Properties of Zirconia Suspension with Added Silane Coupling Agent for Additive Manufacturing Processes, *Materials* 15 (4) (2022) 1337.
- [100] P. Yang, et al., Digital light processing 3D printing of surface-oxidized Si3N4 coated by silane coupling agent, *J. Asian Ceram. Soc.* 10 (1) (2022) 69–82.
- [101] K. Sengloyluan, et al., Synergistic Effects in Silica-Reinforced Natural Rubber Compounds Compatibilised by ENR in Combination with Different Silane Coupling Agent Types, *J. Rubber Res.* 19 (3) (2016).
- [102] C.Y.K. Lung, J.P. Matlinlinna, Aspects of silane coupling agents and surface conditioning in dentistry: an overview, *Dent. Mater.* 28 (5) (2012) 467–477.
- [103] I.U. Perera, et al., 3D-printed refractive secondary optics for LED lighting. 3D Printing for Lighting, SPIE, 2023.
- [104] Y. Xu, et al., Low-Cost Volumetric 3D Printing of High-Precision Miniature Lenses in Seconds, *Adv. Opt. Mater.* 10 (17) (2022) 2200488.
- [105] X. Chen, et al., High-speed 3D printing of millimeter-size customized aspheric imaging lenses with sub 7 nm surface roughness, *Adv. Mater.* 30 (18) (2018) 1705683.
- [106] C. Yuan, et al., Ultrafast three-dimensional printing of optically smooth microlens arrays by oscillation-assisted digital light processing, *ACS Appl. Mater. Interfaces* 11 (43) (2019) 40662–40668.
- [107] F. Alam, et al., 3D printed intraocular lens for managing the color blindness, *Addit. Manuf. Lett.* 5 (2023) 100129.
- [108] S. Ristok, et al., Stitching-free 3D printing of millimeter-sized highly transparent spherical and aspherical optical components, *Opt. Mater. Express* 10 (10) (2020) 2370–2378.
- [109] B. Li, et al., Femtosecond laser 3D printed micro objective lens for ultrathin fiber endoscope, *Fundam. Res.* (2022).
- [110] K.C. Kiekens, J.K. Barton, 3D printed lens for depth of field imaging, *OSA Contin.* 2 (11) (2019) 3019–3025.
- [111] J. Li, et al., 3D-Printed Micro Lens-in-Lens for In Vivo Multimodal Microendoscopy, *Small* 18 (17) (2022) 2107032.
- [112] M. Ali, et al., 3D-Printed Holographic Fresnel Lenses, *Adv. Eng. Mater.* 24 (9) (2022) 2101641.
- [113] F. Alam, et al., 3D printed contact lenses for the management of color blindness, *Addit. Manuf.* 49 (2022) 102464.
- [114] A.E. Salih, et al., Low-cost customized color-blind contact lenses using 3D printed molds, *Adv. Eng. Mater.* (2023) 2300004.
- [115] M. Treacy, Dynamical diffraction in metallic optical gratings, *Appl. Phys. Lett.* 75 (5) (1999) 606–608.
- [116] T. Guo, et al., Plasmonic optical fiber-grating immunosensing: a review, *Sensors* 17 (12) (2017) 2732.
- [117] Y. Zhu, et al., Recent advancements and applications in 3D printing of functional optics, *Addit. Manuf.* 52 (2022) 102682.
- [118] Z. Hong, et al., Three-dimensional printing of glass micro-optics, *Optica* 8 (6) (2021) 904–910.
- [119] J. Purtov, et al., Nanopillar diffraction gratings by two-photon lithography, *Nanomaterials* 9 (10) (2019) 1495.
- [120] L.D. Vallejo Melgarrejo, et al., Manufacture of lenses and diffraction gratings using DLP as an additive manufacturing technology, *Smart Materials, Adaptive Structures and Intelligent Systems*, American Society of Mechanical Engineers, 2018.
- [121] H. Ma, A.Y. Jen, L.R. Dalton, Polymer-based optical waveguides: materials, processing, and devices, *Adv. Mater.* 14 (19) (2002) 1339–1365.
- [122] H. Kogelnik, Theory of optical waveguides, in: *Guided-wave optoelectronics*, Springer, 1990, pp. 7–88.
- [123] R.A. Potyrailo, S.E. Hobbs, G.M. Hieftje, Optical waveguide sensors in analytical chemistry: today's instrumentation, applications and trends for future development, *Fresenius' J. Anal. Chem.* 362 (1998) 349–373.
- [124] K. Ng, et al., Single-mode SU-8 waveguide fabricated using ultrafast direct laser writing, *Optik* 270 (2022) 170068.
- [125] F. Frascella, et al., Three-dimensional printed photoluminescent polymeric waveguides, *ACS Appl. Mater. Interfaces* 10 (45) (2018) 39319–39326.
- [126] M. Schumann, et al., Hybrid 2D–3D optical devices for integrated optics by direct laser writing, *Light.: Sci. Appl.* 3 (6) (2014) e175–e175.
- [127] N. Hodgson, H. Weber, applications, in: *Optical resonators: fundamentals, advanced concepts*, Vol. 108, Springer Science & Business Media, 2005.
- [128] Y. Li, et al., Integrative optofluidic microcavity with tubular channels and coupled waveguides via two-photon polymerization, *Lab a Chip* 16 (22) (2016) 4406–4414.
- [129] Z.-P. Liu, et al., Direct laser writing of whispering gallery microcavities by two-photon polymerization, *Appl. Phys. Lett.* 97 (21) (2010).
- [130] Z. Li, et al., Femtosecond laser microprinting of a fiber whispering gallery mode resonator for highly-sensitive temperature measurements, *J. Light. Technol.* 37 (4) (2019) 1241–1245.
- [131] S. Zhang, et al., High-Q polymer microcavities integrated on a multicore fiber facet for vapor sensing, *Adv. Opt. Mater.* 7 (20) (2019) 1900602.
- [132] A.S. Kuenstler, et al., Vat Photopolymerization Additive Manufacturing of Tough, Fully Recyclable Thermosets, *ACS Appl. Mater. Interfaces* 15 (8) (2023) 11111–11121.
- [133] A. Malas, et al., Fabrication of high permittivity resin composite for vat photopolymerization 3D printing: Morphology, thermal, dynamic mechanical and dielectric properties, *Materials* 12 (23) (2019) 3818.
- [134] M. FARSAARI, B.N. CHICHKOV, Two-photon fabrication: Technology focus: organic photonics, *Nat. Photonics (Print.)* 3 (8) (2009) 450–452.
- [135] Z. Xu, et al., Vat photopolymerization of fly-like, complex micro-architectures with dissolvable supports, *Addit. Manuf.* 47 (2021) 102321.
- [136] T.Y. Kim, S.-H. Park, K. Park, Development of functionally graded metamaterial using selective polymerization via digital light processing additive manufacturing, *Addit. Manuf.* 47 (2021) 102254.
- [137] J. Lu, et al., Vat photopolymerization 3D printing gyroid meta-structural SiOC ceramics achieving full absorption of X-band electromagnetic wave, *Addit. Manuf.* 78 (2023) 103827.
- [138] S.M. Montgomery, et al., Recent advances in additive manufacturing of active mechanical metamaterials, *Curr. Opin. Solid State Mater. Sci.* 24 (5) (2020) 100869.
- [139] S.M. Montgomery, et al., Locally patterned anisotropy using grayscale vat photopolymerization, *Addit. Manuf.* 73 (2023) 103687.
- [140] D. Cygas\*, et al., Monitoring the mechanical and structural behavior of the pavement structure using electronic sensors, *Comput. -Aided Civ. Infrastruct. Eng.* 30 (4) (2015) 317–328.
- [141] J. Wang, et al., Applications of optical fiber sensor in pavement Engineering: A review, *Constr. Build. Mater.* 400 (2023) 132713.
- [142] L.T. Geng, et al., Application of FBG sensors in flexible pavement monitoring, *Adv. Mater. Res.* 255 (2011) 3397–3403.
- [143] S. Shen, et al., Fiber-optic water pressure sensor fabricated by a 3D printing technique, *Advanced Sensor Systems and Applications IX*, SPIE, 2019.
- [144] R.K. Poduval, et al., 3D printed micro-scale fiber optic probe for intravascular pressure sensing, *Biosensing and Nanomedicine XI*, SPIE, 2018.
- [145] M. Zou, et al., Measurement of Interfacial Adhesion Force with a 3D-Printed Fiber-Tip Microforce Sensor, *Biosensors* 12 (8) (2022) 629.

- [146] J. Liang, et al., Curing Characteristics of a Photopolymer Resin with Dispersed Glass Microspheres in Vat Polymerization 3D Printing, *ACS Appl. Polym. Mater.* 5 (11) (2023) 9017–9026.
- [147] B. Martin, et al., Degree of cure of epoxy/acrylic photopolymers: Characterization with raman spectroscopy and a modified phenomenological model, *Polym. Eng. Sci.* 58 (2) (2018) 228–237.
- [148] Y.Y.C. Choong, et al., High speed 4D printing of shape memory polymers with nanosilica, *Appl. Mater. Today* 18 (2020) 100515.
- [149] Y. Xu, et al., Effect of Zeolite Fillers on the Photopolymerization Kinetics for Photocomposites and Lithography, *ACS Appl. Polym. Mater.* 1 (11) (2019) 2854–2861.
- [150] Y. Zhang, H. Zhang, X. Zhao, In-situ interferometric curing monitoring for digital light processing based vat photopolymerization additive manufacturing, *Addit. Manuf.* 81 (2024) 104001.
- [151] B. Howard, et al., Relationships between conversion, temperature and optical properties during composite photopolymerization, *Acta Biomater.* 6 (6) (2010) 2053–2059.
- [152] F. Aloui, et al., Refractive index evolution of various commercial acrylic resins during photopolymerization, *Express Polym. Lett.* 12 (11) (2018) 966–971.
- [153] Y. Wang, et al., Printing depth modeling, printing process quantification and quick-decision of printing parameters in micro-vat polymerization, *Mater. Des.* 227 (2023) 111698.
- [154] A. Rudin, P. Choi, *The elements of polymer science and engineering*, Academic press, 2012.
- [155] H. Gong, A.T. Woolley, G.P. Nordin, High density 3D printed microfluidic valves, pumps, and multiplexers, *Lab a Chip* 16 (13) (2016) 2450–2458.
- [156] Y. Li, et al., High-fidelity and high-efficiency additive manufacturing using tunable pre-curing digital light processing, *Addit. Manuf.* 30 (2019) 100889.
- [157] Y. Wang, D. Xue, D. Mei, Projection-based continuous 3D printing process with the grayscale display method, *J. Manuf. Sci. Eng.* 142 (2) (2020) 021003.
- [158] A. Heinrich, et al., Additive manufacturing of optical components, *Adv. Opt. Technol.* 5 (4) (2016) 293–301.
- [159] S. Yin, et al., Cold spray additive manufacturing and repair: fundamentals and applications, *Addit. Manuf.* 21 (2018) 628–650.